

AN ABSTRACT OF THE THESIS OF

Susan Elizabeth Wakeham for the degree of Master of Science

in Oceanography presented on August 5, 1977

Title: PETROCHEMICAL PATTERNS IN YOUNG PILLOW BASALTS

DREDGED FROM JUAN DE FUCA AND GORDA RIDGES

Abstract approved:

Redacted for privacy

Dr. John B. Corliss

Twenty-one major, minor and trace elements have been determined by atomic absorption spectrophotometry and by instrumental neutron activation analysis in sixty pillow basalts dredged from Juan de Fuca (32 samples) and Gorda (28 samples) Ridges. Although the petrography and the major element data suggest that Juan de Fuca Ridge basalts are more differentiated than Gorda Ridge basalts, rare earth elements (REE) and incompatible elements do not vary sympathetically with the major elements. Based on comparative study between two ridge segments by factor analysis, geochemical patterns show that REE and trace element data are not consistent with the fractionation models as suggested by earlier workers. Employing appropriate partition coefficients for different minerals, quantitative trace element patterns have been modelled to evaluate whether fractional crystallization or partial melting has occurred. Most of the

basalts can be genetically related to each other within the dredge haul by fractional crystallization alone. However, Juan de Fuca Ridge basalts cannot be directly related to Gorda Ridge basalts by fractional crystallization, unless partial melting is invoked to explain the observed difference in REE and trace elements between the two ridge segments.

My data suggest that Juan de Fuca Ridge basalts are derived by a slightly larger degree of partial melting as compared to Gorda Ridge basalts so that Gorda Ridge basalts contain higher abundances of K, Ti and REE in the melts prior to the onset of fractional crystallization. In addition, picritic basalts reported in central Juan de Fuca Ridge are derived by even larger degrees of partial melting as compared to other Juan de Fuca Ridge basalts. It is proposed that Juan de Fuca Ridge melts have undergone more extensive low-pressure modifications to such an extent that high Fe-Ti basalts are produced in the southern Juan de Fuca Ridge area. In contrast, Gorda Ridge basalts have undergone less low-pressure modifications and only mildly fractionated basalts are produced.

Petrochemical Patterns in Young Pillow Basalts
Dredged from Juan de Fuca and Gorda Ridges

by

Susan E. Wakeham

A THESIS

submitted to

Oregon State University

in partial fulfillment of
the requirements for the
degree of

Master of Science

Completed August 5, 1977

Commencement June 1978

APPROVED:

Redacted for privacy

Assistant Professor of Oceanography
in charge of major

Redacted for privacy

Acting Dean of School of Oceanography

Redacted for privacy

Dean of Graduate School

Date thesis is presented August 5, 1977

Typed by Margie Wolski for Susan E. Wakeham

ACKNOWLEDGEMENTS

I thank Dr. John B. Corliss for his support, his helpful comments during this project and for his constructive criticisms of this thesis. I also wish to thank Drs. Julius Dasch and Ken Scheidegger for their comments, and Dr. Melvin Cutler, for serving on my committee.

Special thanks are extended to Drs. Bill Leeman, Bob Duncan and Debbie Stakes for their assistance in the preparation of early drafts and for their encouragement during the completion of this thesis.

I am deeply indebted to Christin Chou, Ron Stillinger, Bobbi Conard, Dale Mosby and Mark Wangerin for their tolerance and generosity in the lab. Their technical assistance and information was invaluable to me.

Helpful discussions with fellow and former students, Chris, Nancy, John, Bill, Bob, and Mitch are greatly appreciated. I also extend my appreciation to my typist Margie Wolski and photographer Dave Reinert for their service.

This project was supported in part by a graduate research fellowship from the International Nickel Company and by unsponsored grants from the Computer Center and from the Radiation Center.

TABLE OF CONTENTS

| | |
|--|----|
| INTRODUCTION | 1 |
| Tectonic Setting | 2 |
| Previous Study on Juan de Fuca and Gorda Ridges | 4 |
| SAMPLING AND ANALYTICAL PROCEDURE | 8 |
| RESULTS | 12 |
| Petrographic Analysis | 12 |
| Major Element Chemistry | 14 |
| Trace Element Chemistry | 17 |
| Factor Analysis | 23 |
| I. Intradredge Relationship | 28 |
| II. Interdredge Relationship | 28 |
| DISCUSSION | 37 |
| Theoretical Introduction to Fractional Crystallization Models | 38 |
| Testing of Fractional Crystallization Models Against Relative Trace Element Data | 40 |
| Theoretical Introduction to Partial Melting Models | 49 |
| Testing of Partial Melting Models Against Relative Trace Element Data | 50 |
| CONCLUSIONS | 58 |
| BIBLIOGRAPHY | 61 |
| APPENDICES | |
| A. Analytical Data for Major and Incompatible Elements and CIPW Normative Calculations | 67 |
| B. Analytical Data for Rare Earth Elements | 77 |
| C. Chemical Analyses of Standard Rocks Compared to Published Results | 82 |
| D. Petrographic Analysis | 85 |

LIST OF FIGURES

| <u>Figure</u> | | <u>Page</u> |
|---------------|--|-------------|
| 1 | Magnetic contour map and location of dredge hauls | 5 |
| 2 | (Na ₂ O+K ₂ O)-FeO*-MgO diagram | 16 |
| 3 | REE basalts/REE chondrites normalization plot | 18 |
| 4 | Ni versus Cr covariance diagram | 20 |
| 5 | Sc versus Cu covariance diagram | 21 |
| 6 | Sc versus Co covariance diagram | 22 |
| 7 | Factor analysis | 24 |
| 8 | Split diagram of factor analysis showing N-S trends | 25 |
| 9 | Distribution of phenocrysts in factor analysis | 26 |
| 10a | Intradredge relationship: normalization plots for Juan de Fuca Ridge basalts | 29 |
| 10b | Intradredge relationship: normalization plots for Juan de Fuca Ridge basalts | 30 |
| 10c | Intradredge relationship: normalization plots for Juan de Fuca Ridge basalts | 31 |
| 10d | Intradredge relationship: normalization plots for Gorda Ridge basalts | 32 |
| 10e | Intradredge relationship: normalization plots for Gorda Ridge basalts | 33 |
| 11 | Schematic diagram of factor analysis showing lines of normalization used for interdredge study | 34 |
| 12 | Interdredge relationship: normalization plots | 35 |

List of Figures, continued

| | | |
|-----|---|----|
| 13 | Fractional crystallization model | 43 |
| 14a | Correlation between observed and calculated normalization plots for fractional crystallization model: intradredge study | 45 |
| 14b | Correlation between observed and calculated normalization plots for fractional crystallization model: intradredge study | 46 |
| 15 | Correlation between observed and calculated normalization plots for fractional crystallization model: interdredge study | 47 |
| 16 | Partial melting models | 52 |
| 17 | Correlation between observed and calculated normalization plots for partial melting model: interdredge study | 53 |

LIST OF TABLES

| <u>Table</u> | | <u>Page</u> |
|--------------|---|-------------|
| 1 | Geological and Geophysical Comparison Between Juan de Fuca and Gorda Ridges | 3 |
| 2 | Location and Depth of Dredge Hauls used for Analysis | 9 |
| 3 | Partition Coefficients used for Fractional Crystallization Model | 41 |
| 4 | Partition Coefficients used for Partial Melting Model | 42 |

PETROCHEMICAL PATTERNS IN YOUNG PILLOW
BASALTS DREDGED FROM JUAN DE FUCA
AND GORDA RIDGES

INTRODUCTION

Variations in chemical composition of mid-ocean ridge basalts are usually attributed to small-scale mechanisms such as shallow fractional crystallization (Vogt and Byerly, 1976; Bryan and Moore, 1977), varying degrees of partial melting (Bryan and Moore, 1977), and chemically variable mantle source regions (Schilling, 1971). The major question that will be dealt with in this paper is: which of these processes or combination of processes is controlling the chemistry of Juan de Fuca and Gorda Ridge basalts?

The present paper supplies more data than was available to earlier workers on these rocks (Kay et al., 1970; Moore, 1970; Barr and Chase, 1974). Additional samples were collected from Juan de Fuca and Gorda Ridges, in regions which had not been sampled previously. This large collection of samples from within a small area of the spreading ridges provide a unique opportunity to investigate the fine-scale compositional variations of lava erupted on the sea floor. It appears that the models of Kay et al. (1970), Vogt and Byerly (1976), and even the petrologic mixing models of Clague and Bunch (1976) for simple fractional crystallization process for Juan de Fuca and Gorda Ridges are not consistent with the observed

differences in the rare earth elements (REE) and other incompatible elements in Juan de Fuca and Gorda Ridge basalts. REE and trace element data are consistent with the origin of these basalts by varying degrees of partial melting in a homogeneous mantle followed by varying degrees of crystallization of the ascending liquids. This model can be demonstrated by showing the differences in chemistry by using factor analysis and by emphasizing the lack of correlation between the trace elements (REE and transition metals) and the major elements which cannot be explained by simple fractional crystallization alone.

Tectonic Setting

Some of the problems concerning the generation of basaltic magmas of Juan de Fuca and Gorda Ridges are related to geophysical and tectonic differences between the two ridge segments (refer to Table 1). Juan de Fuca Ridge is a broad topographic rise consisting of low, elongate hills and valleys, lacking a well-defined median valley (Barr and Chase, 1974). In contrast, Gorda Ridge is characterized by a well-developed median trough similar to Mid-Atlantic Ridge (MAR). Other geophysical parameters used to distinguish the two ridge segments are the seismicity, rate of spreading, and intensity of magnetization. Juan de Fuca Ridge is not seismically active and shows asymmetric spreading pattern (Elvers et al., 1973),

Table 1. Geophysical and Geological Comparison Between Juan de Fuca and Gorda Ridges.

| Data | Juan de Fuca Ridge | Gorda Ridge |
|-------------------------------|---|----------------------------------|
| 1. <u>Magnetic</u> | | |
| a. spreading pattern | asymmetric | symmetric |
| b. spreading rate | 2.9 cm/yr | 1.6 cm/yr |
| c. intensity of magnetization | high intensity | low intensity |
| 2. <u>Seismic</u> | | |
| a. first motion | normal faulting | normal faulting |
| b. seismic activity | aseismic | actively seismic |
| c. refraction | narrow, shallow, low-velocity zone | wide, shallow, low-velocity zone |
| 3. <u>Bathymetric</u> | | |
| | no rift valley with poorly developed flanking hills | well-developed median trough |
| 4. <u>Heat Flow</u> | | |
| | high heat flow | relatively low |
| 5. <u>Gravitational</u> | | |
| | below normal density mantle | below normal density mantle |

References:

Magnetic: Vine (1968), Elvers et al. (1973), Blakely (1974), Detrick and Lynn (1975), Handschumacher (1976), Vogt and Byerly (1976).

Seismic: Shor et al. (1968)

Bathymetry: Barr and Chase (1974)

Heat Flow: Lister (1969, 1970, 1971)

Gravity: Dehlinger et al. (1971)

a higher rate of spreading (2.9 cm/yr: Handschumacher, 1976) and in two places, a high intensity of magnetization (Vogt and Byerly, 1976) (see Figure 1). On the other hand, Gorda Ridge is seismically active and displays a symmetrical spreading pattern, a slower rate (1.6 cm/yr: Blakely, 1974) and only low intensity of magnetization.

Previous Study on Juan de Fuca and Gorda Ridges

Early geochemical studies of Juan de Fuca and Gorda Ridge basalts revealed differences between the two ridge segments. Kay et al. (1970) demonstrated that the rocks of Juan de Fuca Ridge are more fractionated (Fe-enriched) than those of Gorda Ridge. This diversity was considered a result of extensive fractional crystallization of olivine and plagioclase that accounts for the differences in Ca, Al, Fe and Mg.

These chemical variations in the Juan de Fuca Ridge have also been suggested to result from mantle plumes. Citing extensive volcanism and the occurrence of an array of seamounts extending northwest from the ridge as evidence, Morgan (1972) postulated the presence of a mantle plume in the vicinities of Cob and Explorer Seamounts. Using the data of Kay et al. (1970), Vogt and Johnson (1976) also support the idea by stating that high Fe-Ti basalts of Juan de Fuca Ridge are plume related, based on similarities with the high Fe-Ti contents of basalts from the Galapagos Islands and Iceland.

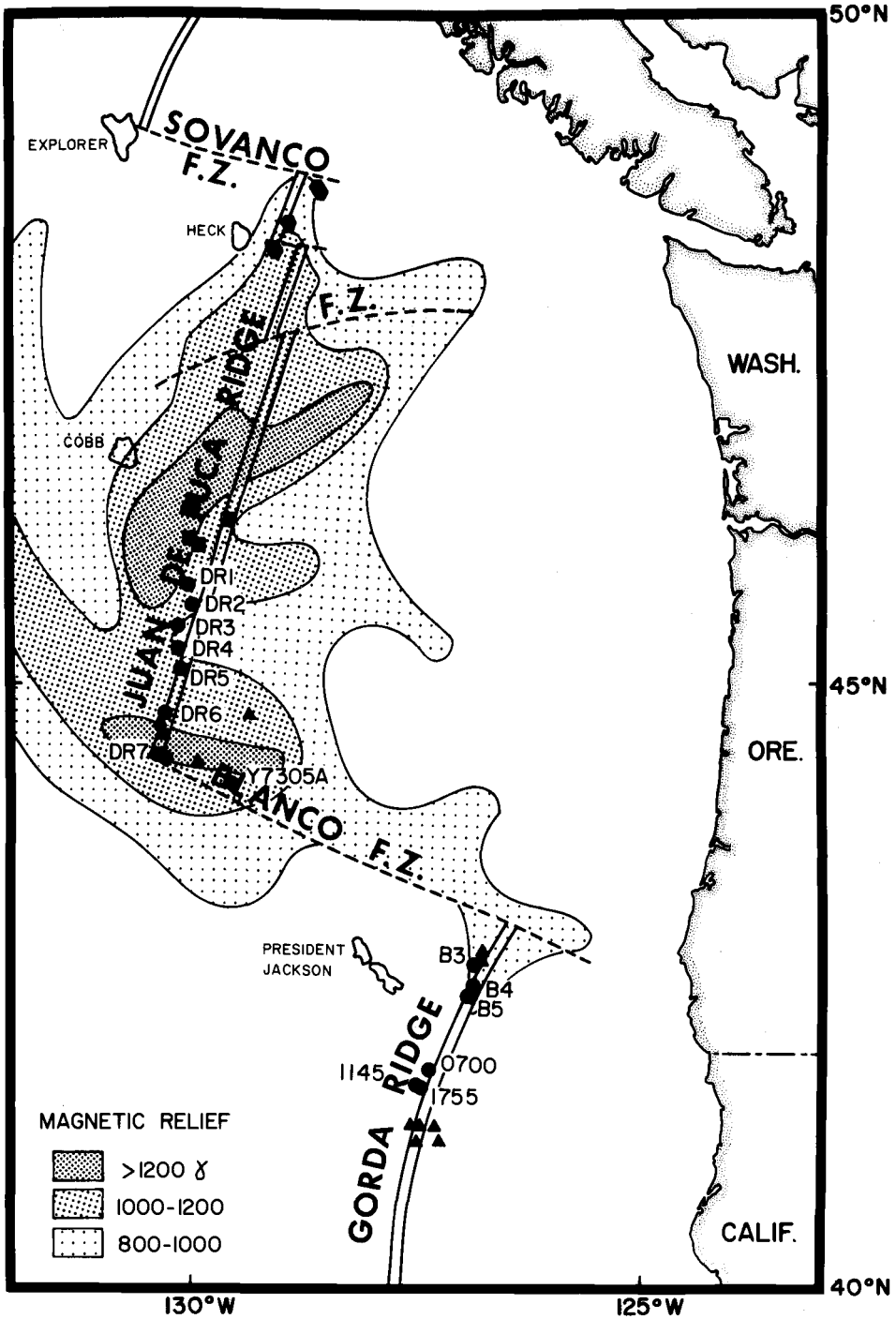


Figure 1. Magnetic contour map including dredge locations.
 ● from Barr and Chase (1974); ■ from Moore (1970);
 ▲ from Kay et al. (1970). All closed circles (●, labelled) are dredge locations for basalts analyzed in this paper.

More recent data, however, suggest that chemical variations occur along a single ridge segment and thus may be controlled by more localized mechanisms. Barr and Chase (1974) dredged more basalts, this time in the northern region of Juan de Fuca Ridge (near Sovanco Fracture Zone) (Figure 1), and found that these basalts are typically high Mg-Ca basalts which are chemically distinct from the Fe-Ti basalts of the southern region. In addition, they emphasized the similarity of high Mg-Ca basalts of Juan de Fuca Ridge with the high Mg-Ca basalts of Gorda Ridge, although the latter have higher K contents. This observation strongly suggests that Juan de Fuca Ridge is not only a ridge chemically distinct from Gorda Ridge as originally proposed by Kay et al. (1970) but also a ridge generating a chemically diverse supply of basalts.

On the basis of seamount studies, Barr (1974) suggested that the geochemical diversity in basalts can be related to two different tectonic frameworks: a mantle plume, and the crustal fracturing that offsets spreading centers. Barr concluded that high Fe-Ti basalts are affected by the presence of a mantle plume (near Cobb Seamount) whereas the high Mg-Ca basalts are typical of ocean ridge influence and are related to crustal fracturing. A conflict still exists, however, between the high Mg-Ca geochemistry of Sovanco Fracture Zone and the high Fe-Ti geochemistry of Blanco Fracture Zone, both of which are generated within a crustal fracturing regime.

Since high Fe-Ti basalts also occur there, it is not feasible to relate only high Mg-Ca basalts to crustal fracturing as Barr has indicated.

Vogt and Byerly (1976) subdivided the high Fe-Ti basalts located in central Juan de Fuca Ridge and fracture-high (magnetic)-amplitude zone (FHAZ) basalts located in the southern Juan de Fuca Ridge. They surmised that the Fe-Ti enrichment is caused primarily by fractional crystallization at shallow depths, rather than by primary mantle plume enrichment in these elements. Then what is the genetic difference (if any) between FHAZ basalts and plume-derived basalts described by Vogt and Byerly (1976)?

The most recent and not completely satisfactory model for the origin of high Fe-Ti basalts of Juan de Fuca Ridge is the computerized petrologic mixing model proposed by Clague and Bunch (1976). Incorporating analytical results from Kay et al. (1970), Moore (1970), and Detrick and Lynn (1975), Clague and Bunch conducted linear least squares approximations using hypothetical phenocryst compositions that match closely with the known phenocryst compositions of the Galapagos Spreading Center and East Pacific Rise. The results from such technique only show that fractional crystallization can produce the observed major element patterns, but do not attempt to explain, and often conflict with trace element data. Major element data need supportive evidence that trace elements and heavy isotope ratios can provide.

SAMPLING AND ANALYTICAL PROCEDURE

The Juan de Fuca Ridge samples were dredged during the Y7305A and Leg I of Y74 cruises aboard R/V Yaquina of Oregon State University. The Gorda Ridge samples were collected during the Y6803 cruise (dredge hauls: 0700, 1145 and 1755) on R/V Yaquina and during the W7605B cruise on R/V Wecoma, also of Oregon State University. Table 2 provides the locations and depth of the dredge hauls used for this study. A majority of the rock was dredged from the central axis of spreading ridges and is thus considered very young in age. Dredge hauls Y74-DR7, Y7305A-1 and Y7305A-4 were collected from the Blanco Fracture Zone located on the southern end of Juan de Fuca Ridge (Figure 1).

A total of 60 samples were selected for chemical analysis. The selection was based on freshness of the samples and on their mineralogy so that a widely diverse group of basalts was chosen to represent each dredge haul. Some criteria used to test for freshness of the samples in order to avoid including altered basalts in the analysis are: megascopic alteration generally in the form of color changes in rock fragments (Hart, 1969) and in the presence of palagonite on glassy margins (Schilling, 1975), H₂O contents, and presence of secondary minerals observed in thin sections. Most of the basalts are apparently fresh throughout and show no color variation and other

Table 2. List of Dredge Hauls from which the Samples were Analyzed, with Corresponding Location and Approximate Depth of Dredging.

| DREDGE HAUL | LOCATION | DEPTH (m) |
|----------------------------|------------------|-----------|
| <u>Juan de Fuca Ridge:</u> | | |
| Y74-1-DR1 | 45°46'N 130°01'W | 2169 |
| Y74-1-DR2 | 45°37'N 129°59'W | 1235 |
| Y74-1-DR3 | 45°27'N 130°08'W | 1250 |
| Y74-1-DR4 | 45°16'N 130°08'W | 2400 |
| Y74-1-DR5 | 45°07'N 130°07'W | 1303 |
| Y74-1-DR6 | 44°45'N 130°17'W | 2251 |
| Y74-1-DR7 | 44°25'N 130°23'W | 1220 |
| Y7305A-RD1 (BFZ) | 44°24'N 130°18'W | 3126 |
| Y7305A-RD4 (BFZ) | 44°11'N 129°33'W | 3354 |
| <u>Gorda Ridge:</u> | | |
| Y6803-DR3 (0700) | 41°52'N 127°21'W | 3200 |
| Y6803-DR4 (1755) | 41°43'N 127°26'W | 2340 |
| Y6803-DR6 (1145) | 41°43'N 127°28'W | 2200 |
| W7605B-DR3 | 42°44'N 126°46'W | 3000 |
| W7605B-DR4 | 42°33'N 126°51'W | 3666 |
| W7605B-DR5 | 42°28'N 126°55'W | 3694 |

evidence of alteration (ie. secondary minerals). In few cases, palagonite rims and dark alternation bands do occur along the outer margin of the basalts, and these have been avoided during sampling. Results from preliminary water analysis (of 30 samples) show a range of 0.13-0.60% total H_2O in fresh Juan de Fuca and Gorda Ridge basalts. Some samples that display minor amounts of alteration minerals in thin sections register low water contents within the range of 0.18-0.37% H_2O , which compares closely with the 0.2-0.3% range used as a criteria for distinguishing fresh from altered basalts (Hart, 1969; Philpotts et al., 1969). Although I have not analyzed for Cs which is known to be the most sensitive indicator of seawater alteration (Hart, 1969) such study would obviously enhance further discrimination of altered from fresh basalts. In the meantime, all basalts which have been selected for this study are considered to be fresh basalts.

The samples were prepared by cutting out small cubes (approx. 50 grams) from the rock and crushed to 100 mesh with an aluminum oxide jaw crusher and disc pulverizer. The crushed whole-rock samples were then split to approximately 400 mg., dissolved in aqua-regia and hydrofluoric acid in teflon bombs according to the procedures given by Fukui (1976), and analyzed by atomic absorption spectrophotometry for Si, Al, Ca, Mg, Ti, K, Cu and Ni. Following the general procedure of Gordon et al. (1968), whole rock samples

were also analyzed by instrumental neutron activation analysis for Na, Fe, La, Ce, Sm, Eu, Tb, Yb, Lu, Hf, Sc, Cr and Co after irradiation in the Oregon State University Triga Mark III Research reactor. The analytical results for each samples are listed in Appendices A and B. The accuracy of the data is indicated by analysis of the USGS standards, W1 and BCR, and laboratory standards, SD0895 and MS1519 (Appendix C).

Normative mineralogy is calculated from the major element chemistry after adjustment of the $\text{Fe}^{+3}/(\text{Fe}^{+2} + \text{Fe}^{+3})$ ratio to 0.111, P_2O_5 content to 0.20, and MnO content to 0.19. These values are taken from an average of fresh mid-ocean ridge basalts (Kay et al., 1970; Moore, 1970; Barr and Chase, 1974). The CIPW norm results are tabulated along with the analytical results (Appendix A).

The analytical data were also subjected to Q-mode factor analysis (Imbrie and Kipp, 1971). Factor analysis is a statistical technique that describes most of the variance in a complex data set in terms of a few, statistically independent variables. Results of chemical analyses from other sources would have been invaluable in this factor analysis; however, data of Kay et al. (1970) does not include Tb, Lu, Hf, Cu, Cr and Co; Moore (1970) and Barr and Chase (1974) do not report data for REE or transition metals; and Corliss (1970) reports no data for Cu, Ni, Ti and K. Because of their incomplete set of data, I could not compare these data with my own in factor analysis.

RESULTS

Petrographic Analysis

In general, the petrography of basalts from the Juan de Fuca and Gorda Ridges is very similar (see Appendix D). Most of the samples are fresh pillow basalts rimmed with glassy margins; few are holocrystalline, angular basalts. They are fairly vesicular, are slightly porphyritic with phenocrysts of olivine and plagioclase, and show typical variolitic and rapidly quenched textures identical to the description summarized by Bryan (1972). Plagioclase microlites occur in the groundmass of all samples and appear to vary in abundance with the rate of cooling as reflected by the degree of quenching.

Large plagioclase and olivine phenocrysts (possible xenocrysts of cognate origin) are more abundant in Gorda Ridge samples than in Juan de Fuca Ridge samples. The appearance of partial resorption in both plagioclase and olivine phenocrysts and oscillatory zoning in several of plagioclase microphenocrysts is common, suggesting continuous reaction with the liquid at higher temperatures and pressures.

Plagioclase and olivine microphenocrysts are more abundant in Juan de Fuca Ridge basalts than in Gorda Ridge basalts. Crystallization of olivine and plagioclase is consistent with the fractionation model developed for oceanic ridge basalts (Shido et al., 1971;

Frey et al., 1974; Bryan and Moore, 1977). Precipitation of these phases causes the residual magma to migrate along the PL-OL cotectic curve in the direction of increasing pyroxene component along the curve. As crystallization proceeds, the residual liquid increases in FeO^*/MgO , and at the eutectic point clinopyroxene joins olivine and plagioclase as phenocryst phases. Larger proportions of olivine and plagioclase microphenocrysts in Juan de Fuca Ridge basalts suggest that Juan de Fuca Ridge samples have undergone longer crystallization history than the Gorda Ridge samples.

The common appearance of pyroxene microphenocrysts in Juan de Fuca Ridge samples reflects advanced stage of crystal fractionation because the residual liquid has reached the eutectic point, where clinopyroxene begins to crystallize.

Another important observation worth noting is a unique occurrence of picritic basalts from Juan de Fuca's dredge haul Y74-DR3. Samples Y74-3-5, 3-13 and 3-29 differ from both Juan de Fuca and Gorda Ridge basalts by the appearance of abundant rounded olivine phenocrysts surrounded by translucent brown chrome-rich spinels. These spinels are abundant where olivine is apparently the only principal silicate phenocryst. Only a few rocks (for example, Y74-5-3, Y74-5-10, Y7305A-4-16, W7605B-3-6, W7605B-5-10, 1145K) contain phenocrysts of both spinel and clinopyroxene. The occurrence of chrome spinel has been reported in Mid-Atlantic

basalts by Frey et al. (1974), Melson and Thompson (1970), and Bryan and Moore (1977). Compositionally, they are similar to spinels from spinel peridotite nodules (Irvine, 1967) which are thought to be representative of the mantle source. If the picritic liquids have equilibrated with the spinel peridotitic source during partial melting, then Y74-DR3 liquids represent relatively undifferentiated nature of this type of basalt, even though they may have already undergone limited olivine fractionation since their formation by partial melting. These picritic samples contain large amounts ($> 12\%$) of normative olivine.

Dredge haul Y74-DR3 also differ by being the least vesicular set of samples. This observation may reflect a relatively low content of volatile components in these lavas.

Major Element Chemistry

Analytical results tabulated in Appendix A demonstrate that the chemistry of both Juan de Fuca and Gorda Ridge basalts is consistent with the chemistry of basalts reported by Kay et al. (1970), Moore (1970), and Barr and Chase (1974). Basalts from dredge hauls Y74-DR6, Y74-DR7 and Y7305A-1 reflect high Fe-Ti content of the southern Juan de Fuca Ridge, similar to those reported by Detrick and Lynn (1975) and Vogt and Byerly (1976). The remaining basalts (in Juan de Fuca Ridge north of the high Fe-Ti region and in Gorda

Ridge) are more typical of the differentiated olivine-plagioclase tholeiites reported in Mid-Atlantic Ridge (Engel et al., 1965; Hekinian et al., 1976; Bryan and Moore, 1977). However, picrites from dredge haul Y74-DR3 approach the chemistry more typical of Mg-Ca basalts, with very low TiO_2 and K_2O contents accompanied by low FeO^*/MgO ratio, and are similar to the Mg-Ca basalts of the northern region of Juan de Fuca Ridge (Barr and Chase, 1974). Furthermore, comparisons of analyses from Juan de Fuca Ridge with analyses from Gorda Ridge indicated that the latter are more similar to the basalts from the northern region of Juan de Fuca Ridge, although the alkali contents are generally greater.

The difference between the two ridge segments is more readily illustrated in the $(\text{Na}_2\text{O} + \text{K}_2\text{O})$ - FeO^* - MgO diagram (Figure 2). The elongation of the trend is parallel to the direction of tholeiitic trends of magmatic differentiation (Miyashiro et al., 1970) and thus represents this process. Gorda Ridge samples display slight systematic enrichment in the alkalis which may reflect the accumulation of plagioclase phenocrysts in these samples. However, plagioclase in this rock type contains very small amount of alkalis (Carmichael et al., 1974) and enrichment in the alkalis may reflect differences in magma chemistry instead. It is also important to recognize that abundant accumulation of olivine and plagioclase phenocrysts in Gorda Ridge samples will also bias the whole rock analyses toward

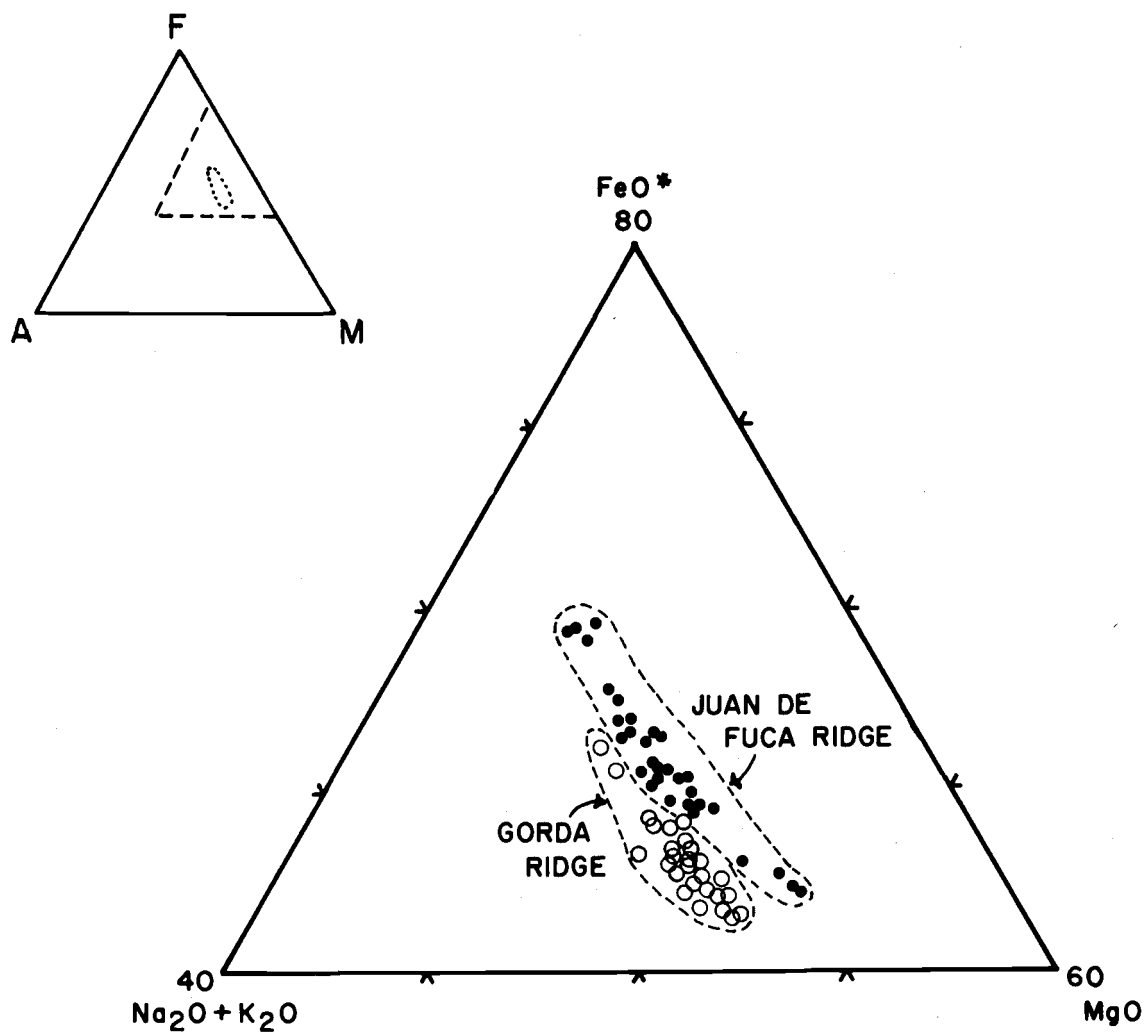


Figure 2. AFM diagram taken from the insert shown in upper left hand corner.

higher Al and Mg contents, thus pushing the Gorda Ridge samples more closely toward the MgO apex. However, one shall quickly observe random distribution of these phenocrysts in factor analyses (see below) which suggests that other elements exert strong influence on the chemical relationship and that this relationship is independent of the effect of phenocrysts; for example, the difference in composition may have developed during the partial melting episode that formed these respective magmas.

Trace Element Chemistry

REE abundances were normalized against chondrites (Haskins et al., 1967) and plotted in Figure 3. The observed depleted light REE profiles are typical of the REE profiles for mid-ocean ridge basalts (Schilling, 1975; Bryan et al., 1976). Basalts of this type may have been derived from depleted, low velocity layer material, considered to be a residue for previous partial melting episodes (Gast, 1968). The REE profiles indicate even stronger depletion in the light REE relative to the heavy REE in dredge haul Y74-DR3 whose picritic samples are plotted individually to show detailed variations.

It is interesting to note that the range found in Gorda Ridge basalts completely overlaps the range in Juan de Fuca Ridge basalts. This observation is not consistent with Kay et al.'s (1970) contention

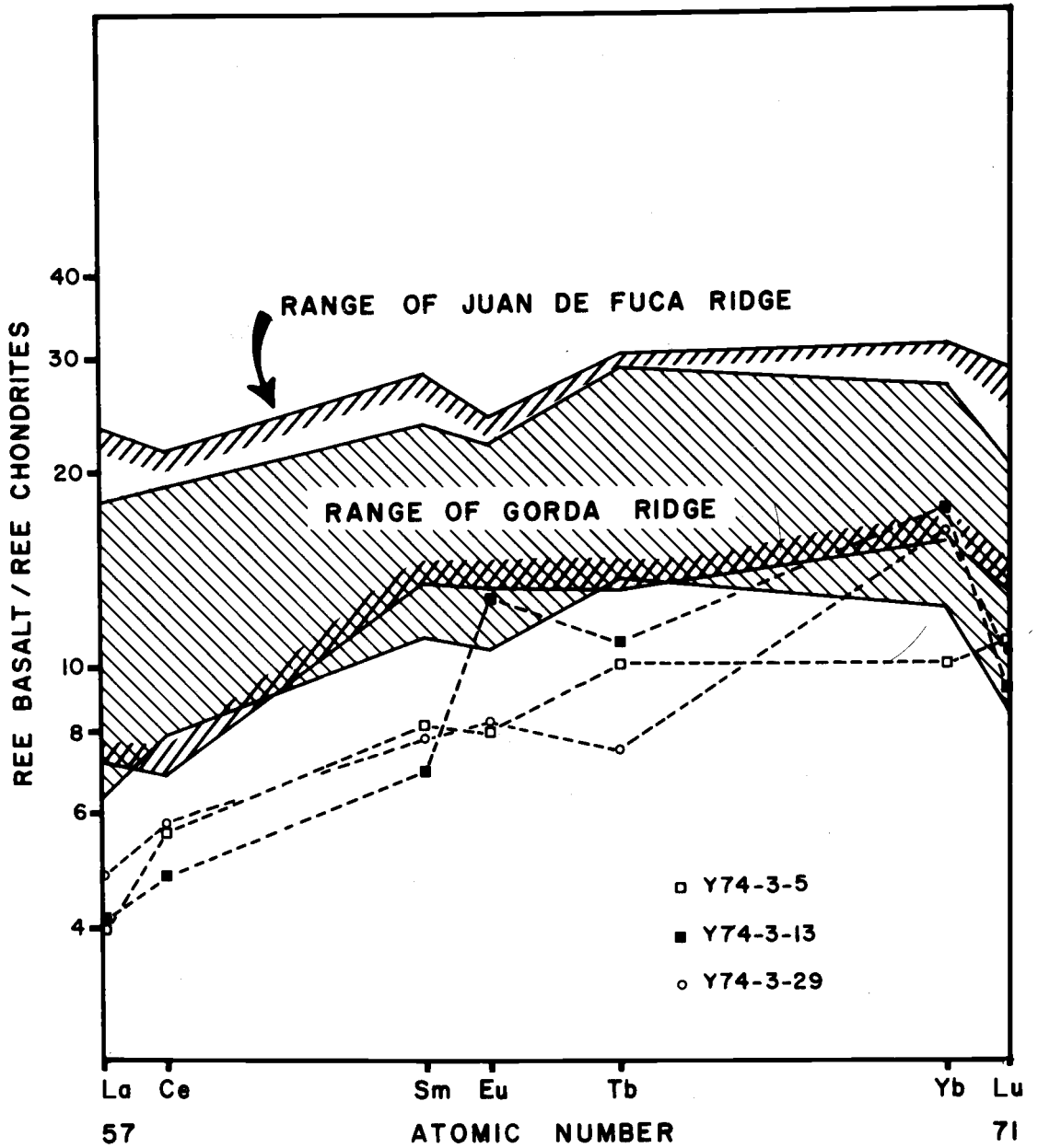


Figure 3. Chondrite normalization plots. The three lines show variation of three picritic samples from dredge haul Y74-DR3.

that Juan de Fuca Ridge basalts are more REE enriched than Gorda Ridge basalts. Furthermore, in terms of only the AFM diagram, Juan de Fuca Ridge basalts appear to be more fractionated (Fe-enriched) than Gorda Ridge basalts. In terms of only the petrographic analysis, Juan de Fuca Ridge basalts again appear to be more fractionated than Gorda Ridge basalts. The REE are thought to be more enriched with increasing extent of crystal fractionation (Gast, 1968; Schilling and Bonatti, 1975); therefore, the basalts of Juan de Fuca Ridge are expected to display more enriched total REE profiles than the basalts of Gorda Ridge. It appears that the REE compositions do not vary sympathetically with the major elements nor with the petrographic analysis.

Juan de Fuca Ridge basalts also differ from Gorda Ridge basalts in terms of the transition metals. Figure 4-6 contrast compositional characteristics among the dredge hauls. In general, Gorda Ridge basalts are more enriched in Cr and Ni and more depleted in Sc and Co than the Juan de Fuca Ridge basalts. The Cr and Ni abundances appear to be sensitive to the presence of spinel and olivine phenocrysts in the samples. This can be readily observed in some picritic samples whose extremely high Cr and Ni contents are reflected by the appearance of spinel and olivine phenocrysts. The abundances of Cu (see Figure 5) are similar for both ridge segments with the exception of Y74-DR1, -DR2 and -DR3, which show higher

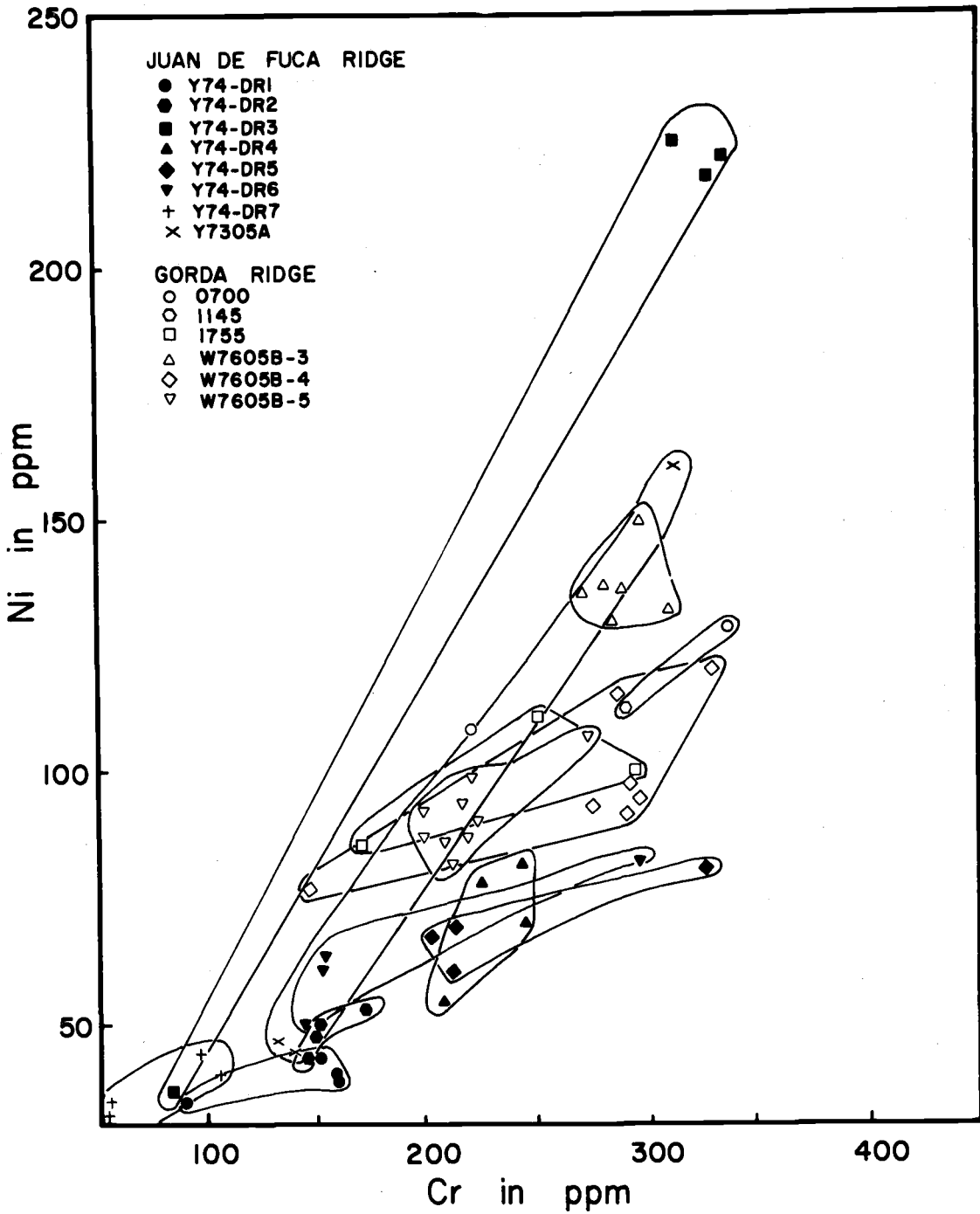


Figure 4. Ni versus Cr covariance diagram.

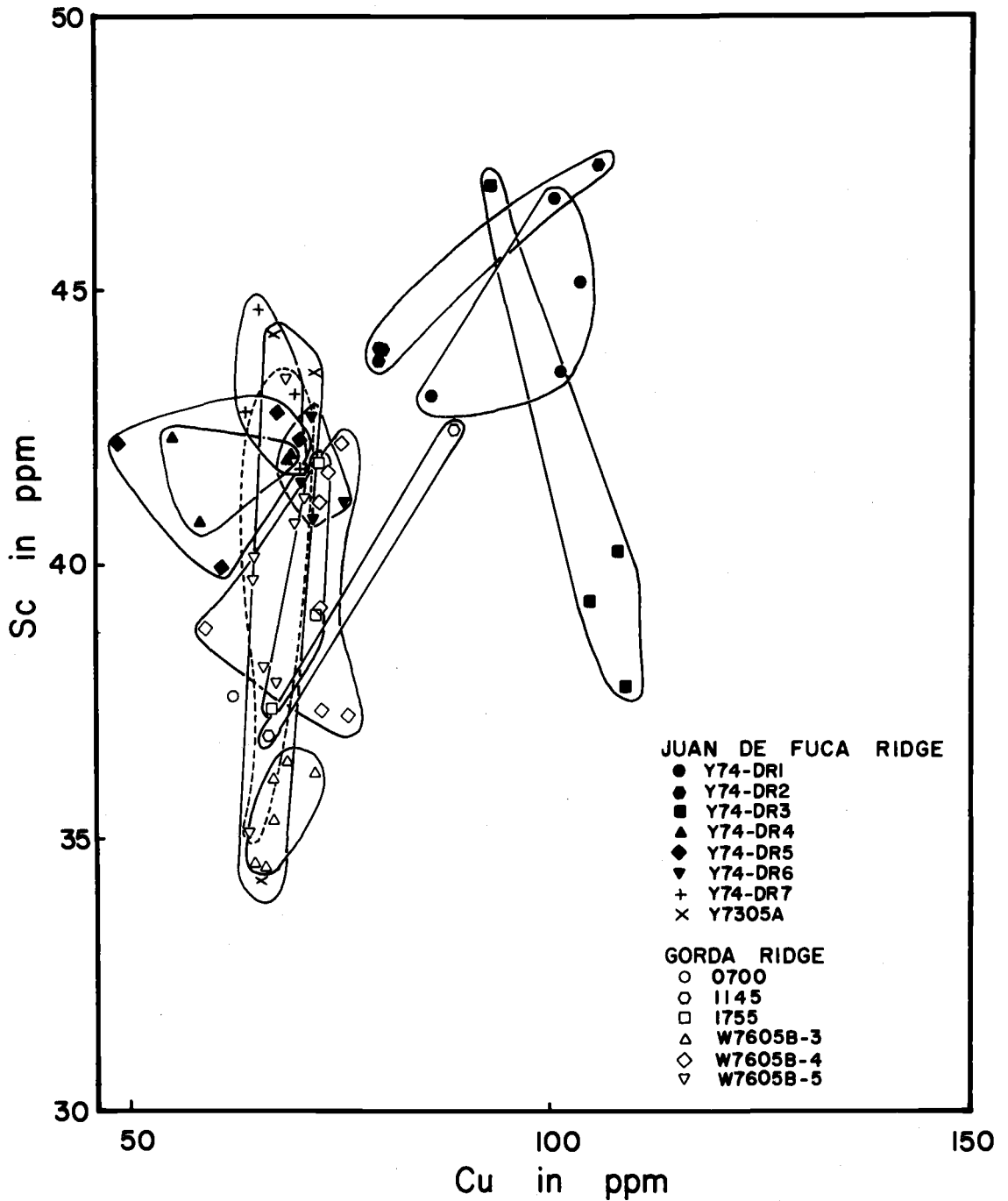


Figure 5. Sc versus Cu covariance diagram. Dashed line is used to facilitate the reader to observe clustering of dredge haul W7605B-5.

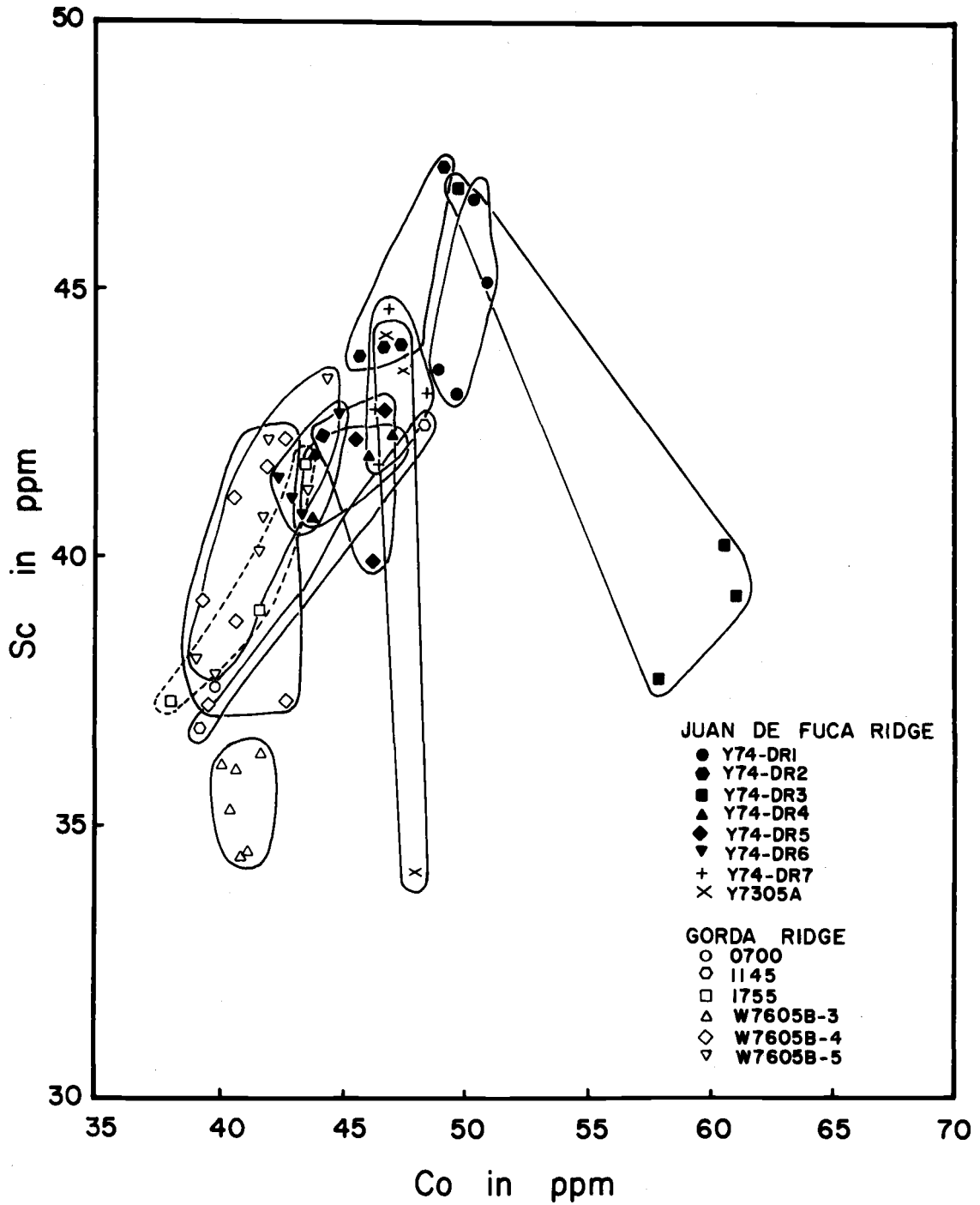


Figure 6. Sc versus Co covariance diagram. Dashed line is used for the same purpose as before, which show clustering of dredge haul 1755.

Cu contents than the rest of the samples.

Factor Analysis

The distinction between Juan de Fuca and Gorda Ridge basalts can be summarized through the statistical technique of factor analysis. Since all the elements which I analyzed are of roughly equal geochemical interest in this study, I scaled the concentration of each element in each sample to the fraction of its concentration range in the data set so that the abundance elements would not dominate the resultant factors as they would if raw data were used. Figure 7 is the result of factor analysis based on 60 samples and 21 variables. Three factors account for 99.5% of the variance in the scaled data. Figure 9 illustrates the distribution of phenocrysts in factor analysis.

According to factor analysis (Figure 8), Juan de Fuca Ridge displays a N-S trend toward Factor 1 that is dominated by an increase in Fe, Ti, REE, K and Na. Gorda Ridge, on the other hand, has a unique trend of its own. Unlike Juan de Fuca Ridge, it displays very little tendency toward Factor 1 and instead has two patterns, both pointing toward Factor 3 that is dominated by an increase in Sc, Ca and Cu and a decrease in REE.

Another way of looking at the trend along the ridge crest is by observing the two distinct groups of data points on the diagram. All

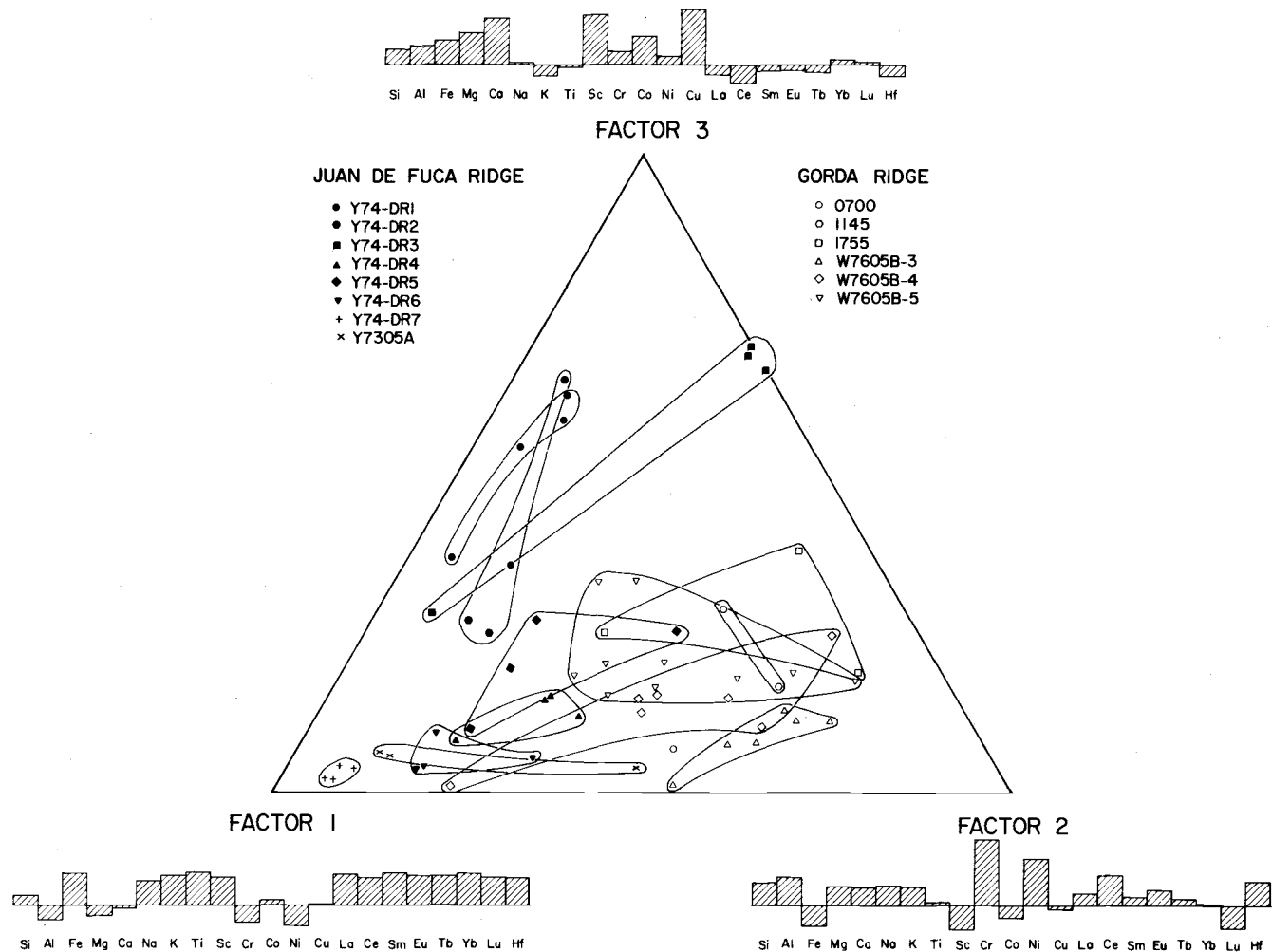


Figure 7. Result of factor analysis. Histograms are scaled varimax factors illustrating the relative significance of the elements. Note the elongated feature of each dredge haul and the spread of the dredge hauls between Factors 2 and 3.

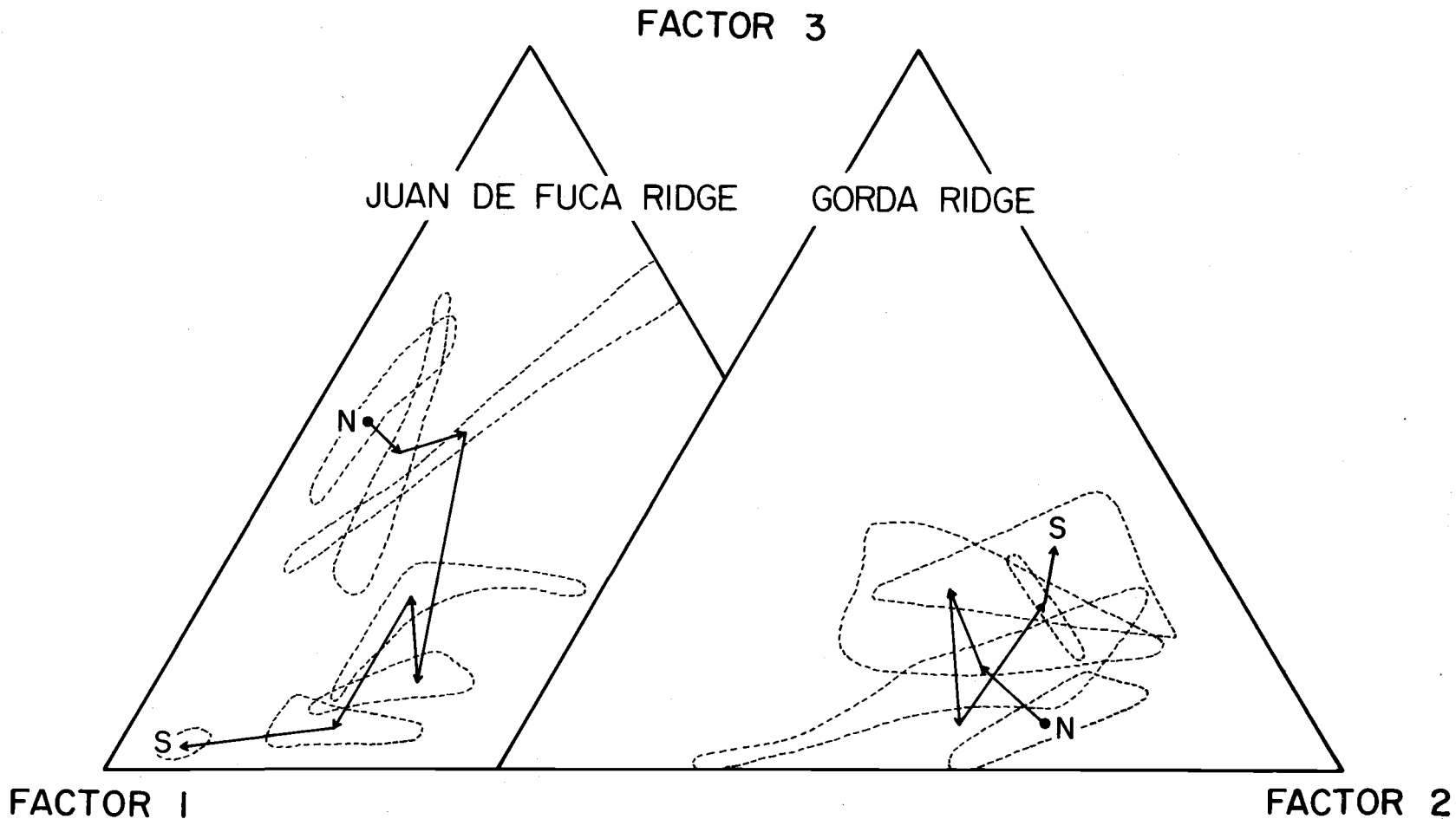


Figure 8. Split diagram for factor analysis used to illustrate distinctive grouping of two ridge segments and the N-S trends of the dredge hauls.

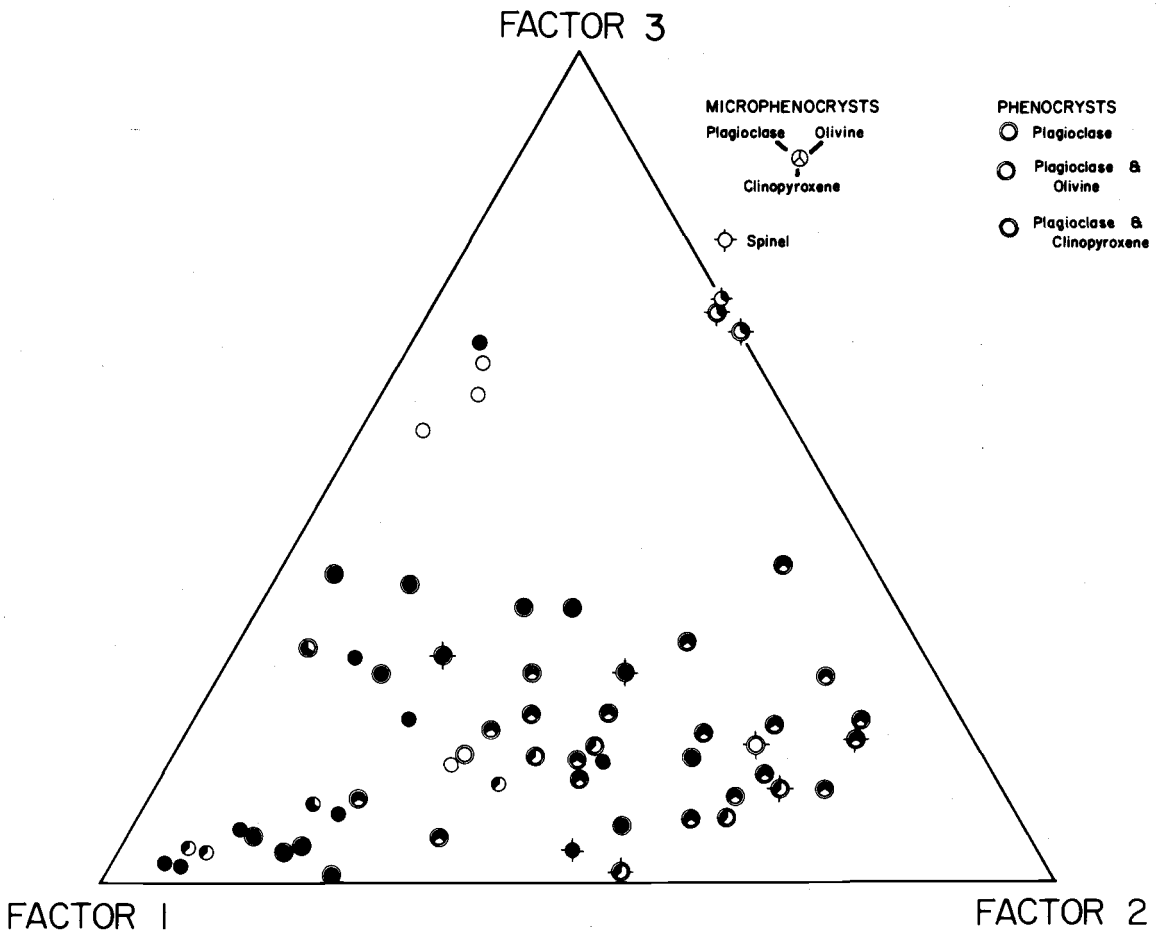


Figure 9. Distribution of phenocrysts in factor analysis. Shaded fraction represents the occurrence of the phenocrysts in the sample. Note particularly the abundances of clinopyroxene phenocrysts toward Factor 1. Plagioclase and olivine phenocrysts are randomly distributed throughout the diagram.

of Juan de Fuca Ridge basalts which represent the northern ridge segment occupy the left portion of the diagram, clustering parallel to the Factor 1-3 edge. All of Gorda Ridge basalts which represent the southern ridge segment have data points that gather close to Factor 2 apex. This compositional difference between two ridge segments implies that chemical diversity is created by markedly different process or processes. The two groups can be quickly thought of as two distinct mantle sources, thus providing explanation for inhomogeneity in the mantle. However, a more rigorous approach can be made by placing petrochemical constraints upon the extent to which REE and transition metals are fractionated during partial melting and during fractional crystallization, thus taking the important assumption that these basalts are derived from a single, uniformly homogeneous mantle source. This will be discussed more thoroughly in the next section.

The next step, then, is to evaluate what inter-elemental changes are taking place between samples within a dredge haul and how a chemical pattern varies from one dredge haul to another. Two significant features are noted in factor analysis (Figure 9): a consistent elongation of each dredge haul toward Factor 1 apex that is dominated by the abundances of Fe, Na, K, Ti, Sc and the REE, and a spread between each dredge haul between Factors 2 and 3 which is dominated by the abundances of Ca, Sc, Cu and inversely the REE.

I. Intradredge Relationship:

To determine what elements account for the elongated feature among the samples within each dredge haul, I have normalized all the samples in a dredge haul against what is believed to be the least differentiated member of that dredge haul. The results of these normalizations (Figure 10) illustrates positive correlation between Fe, K, Na, Ti, Sc and REE and the overall negative correlation between these components and Ca, Mg, Al, Cr, Ni and Co. Qualitatively, these changes could be produced by crystallization of calcic plagioclase along with magnesium-rich olivine (Bryan and Moore, 1971). Positive Eu anomaly occur in all of Juan de Fuca's dredge hauls Y74-DR1, -DR2, -DR3, -DR4, and Y7305A. Furthermore, Juan de Fuca's dredge hauls Y74-DR5, -DR6, -DR7, and Y7305A display much depleted Cr relative to the undifferentiated components of their dredge hauls.

II. Interdredge Relationship:

To determine what elements account for the spread between each dredge haul toward Factor 3 apex, I have also made normalization plots against samples that reside close to Factors 1-2 edge (Figure 12). These samples were chosen arbitrarily in order to demonstrate what trends occur across the diagram toward Factor 3

I. INTRADREDGE STUDY JUAN DE FUCA

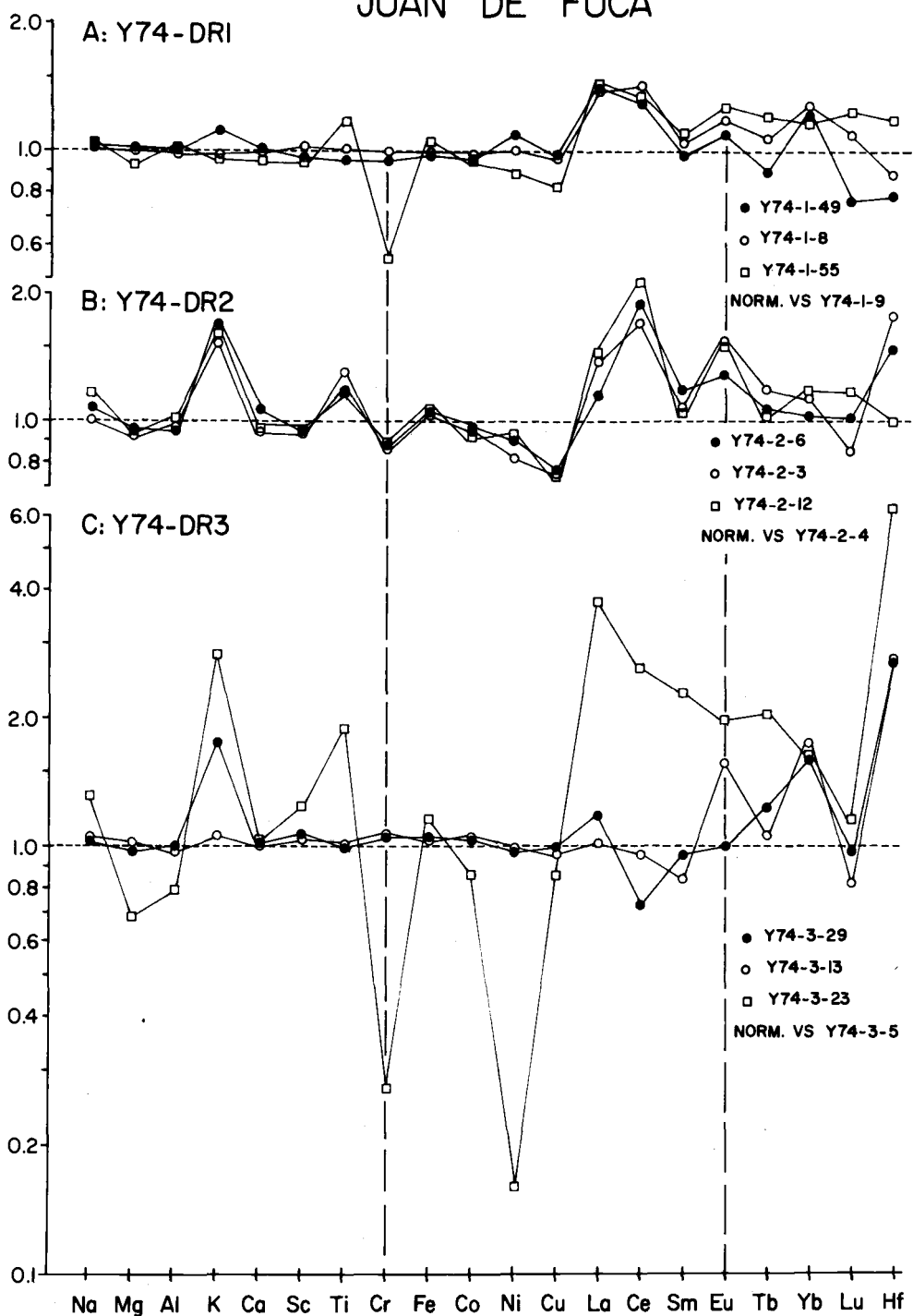


Figure 10a. Normalization plots of samples within dredge hauls Y74-DR1, -DR2 and -DR3.

I. INTRADREDGE STUDY JUAN DE FUCA

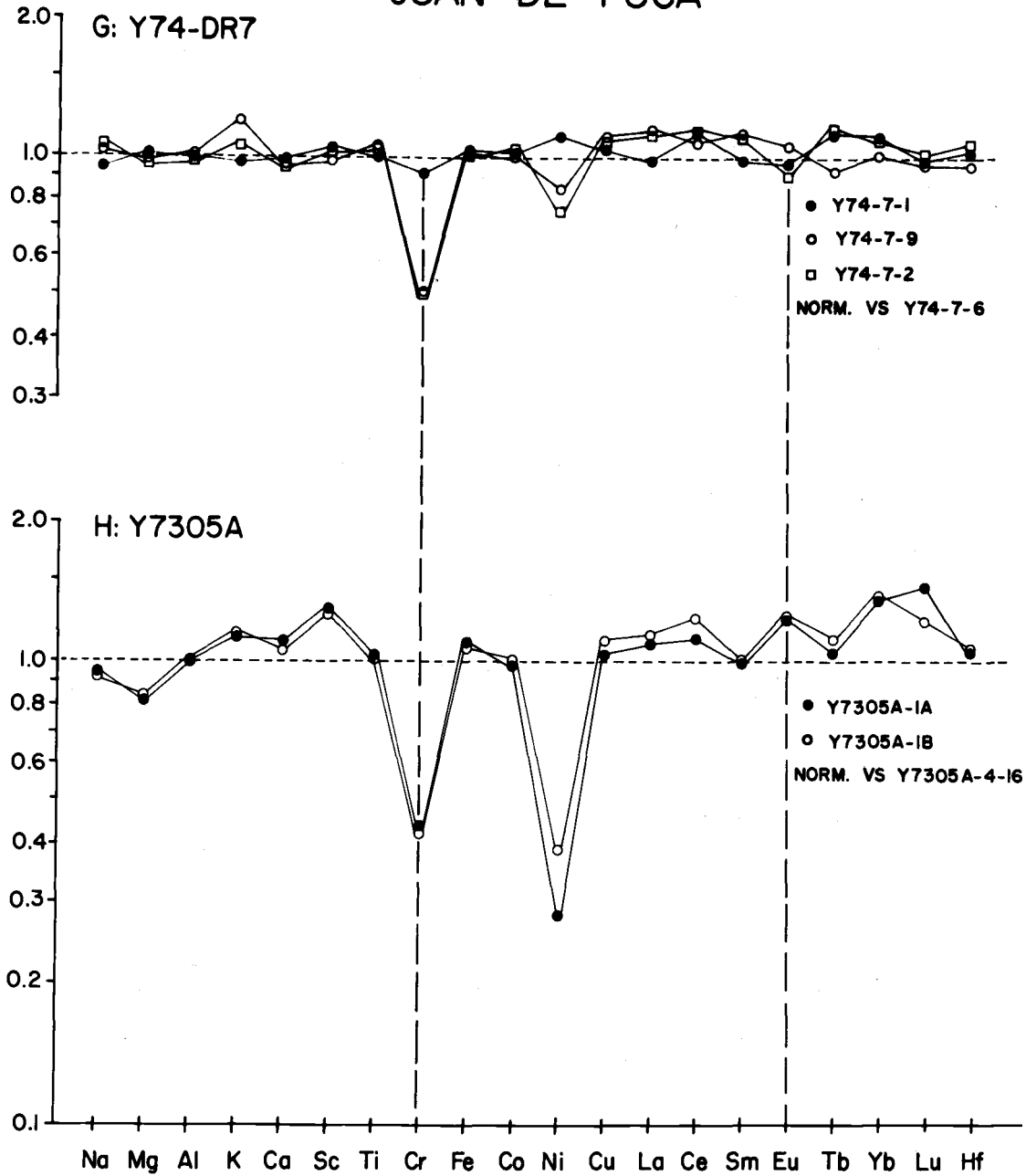


Figure 10c. Normalization plots of samples within dredge hauls Y74-DR7 and Y7305A.

I. INTRADREDGE STUDY JUAN DE FUCA

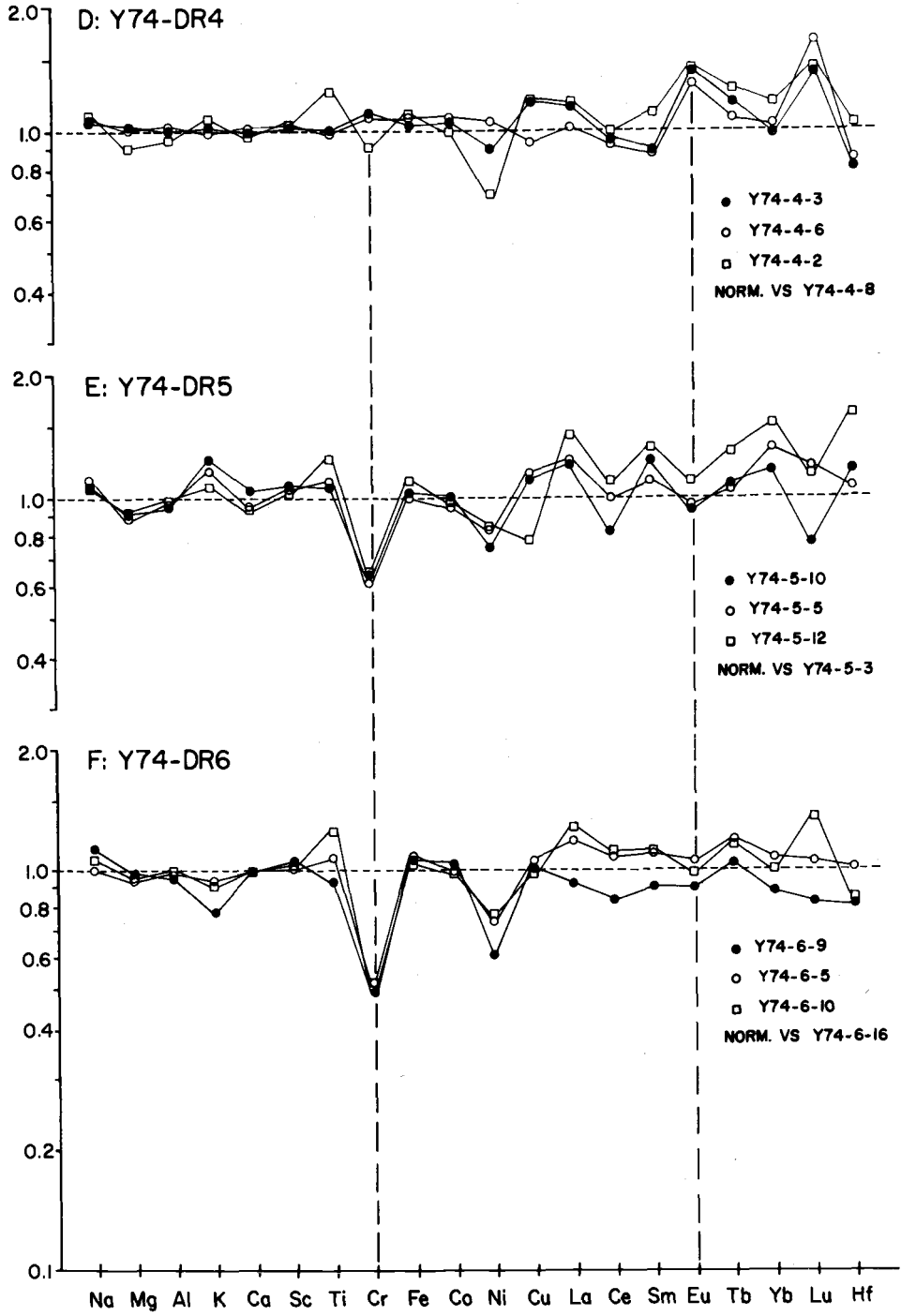


Figure 10b. Normalization plots of samples within dredge hauls Y74-DR4, -DR5 and -DR6.

I. INTRADREDGE STUDY GORDA RIDGE

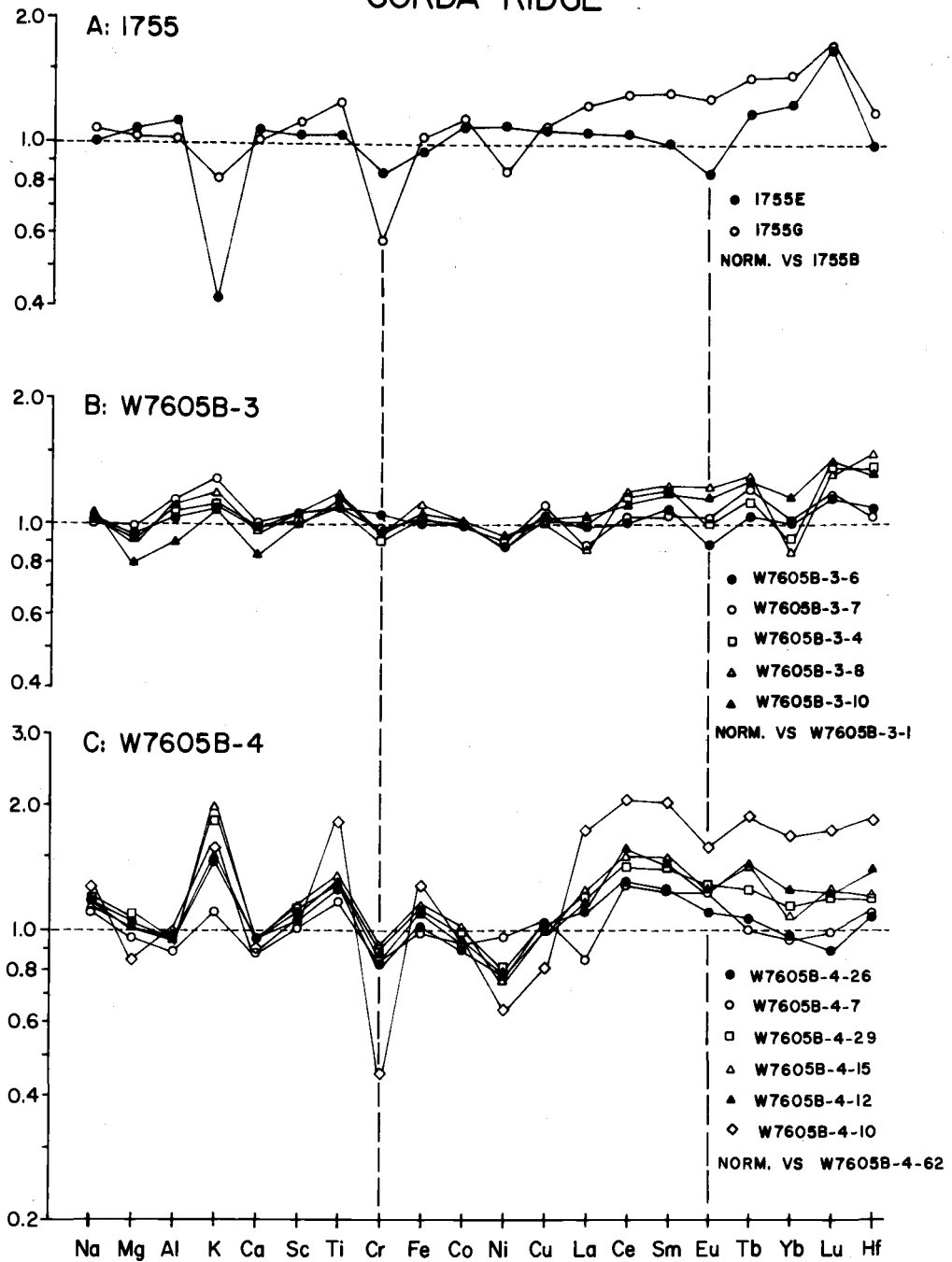


Figure 10d. Normalization plots of samples within dredge hauls 1755, W7605B-3 and B-4.

I. INTRADREDGE STUDY GORDA RIDGE

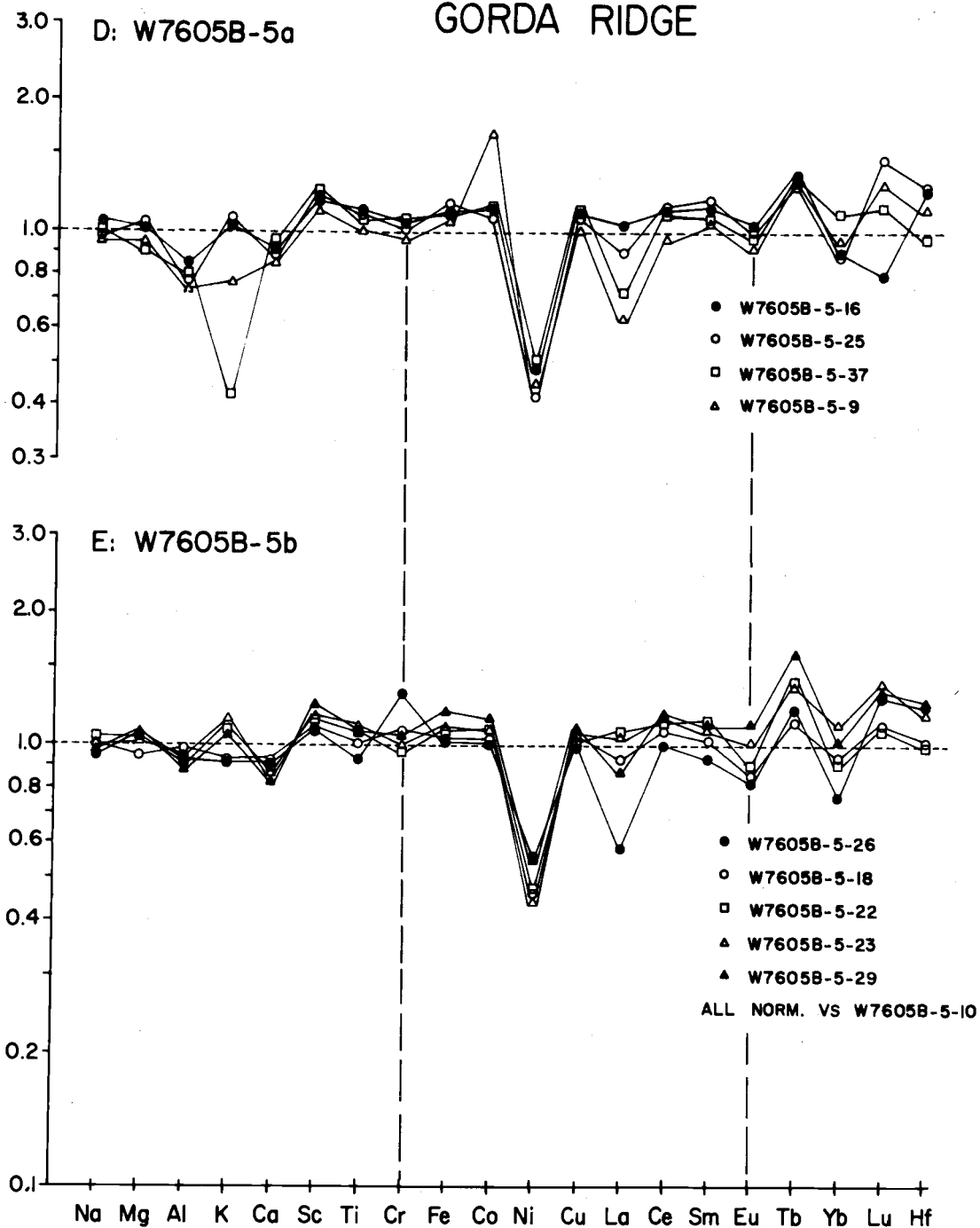


Figure 10e. Normalization plots of samples within dredge hauls W7605B-5.

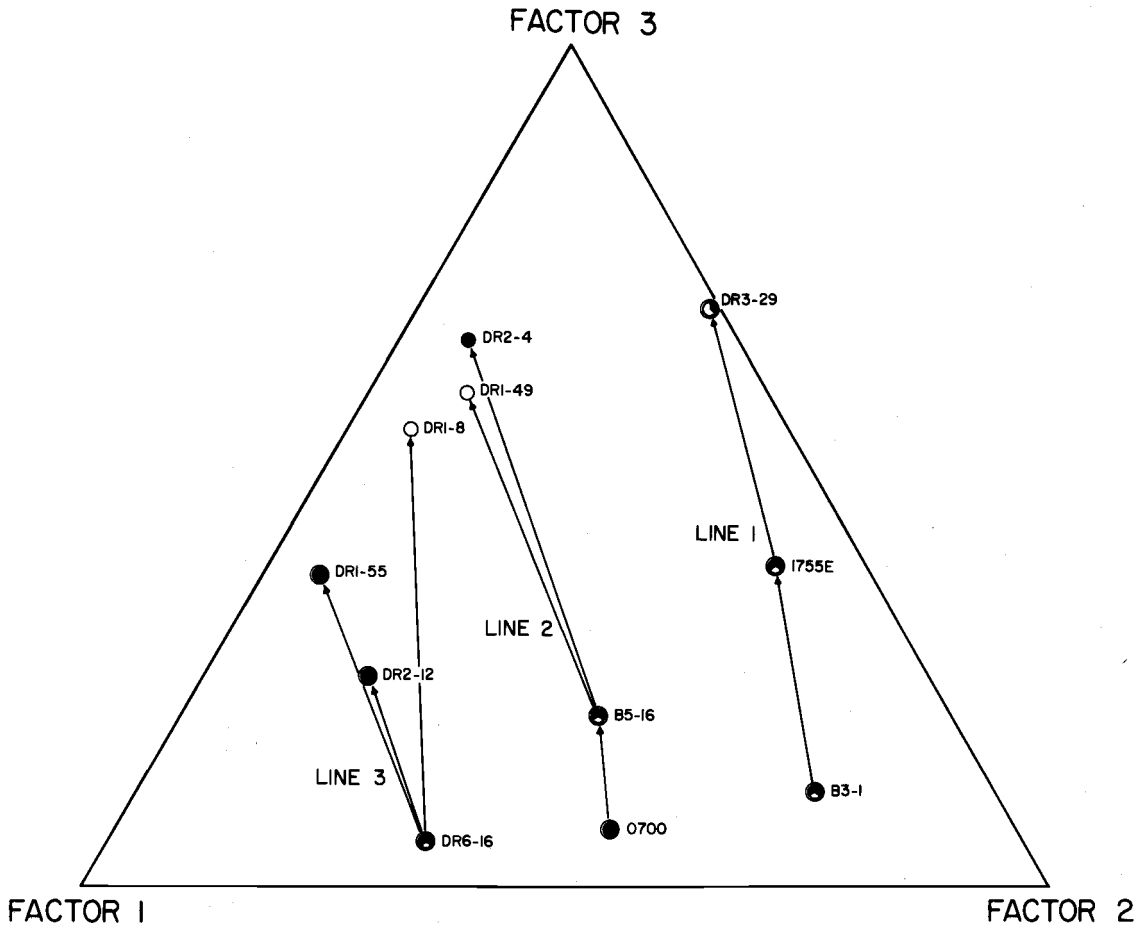


Figure 11. Schematic diagram showing interdredge relationship. Results of normalization along each line are illustrated in Figure 12.

II. INTERDREDGE STUDY

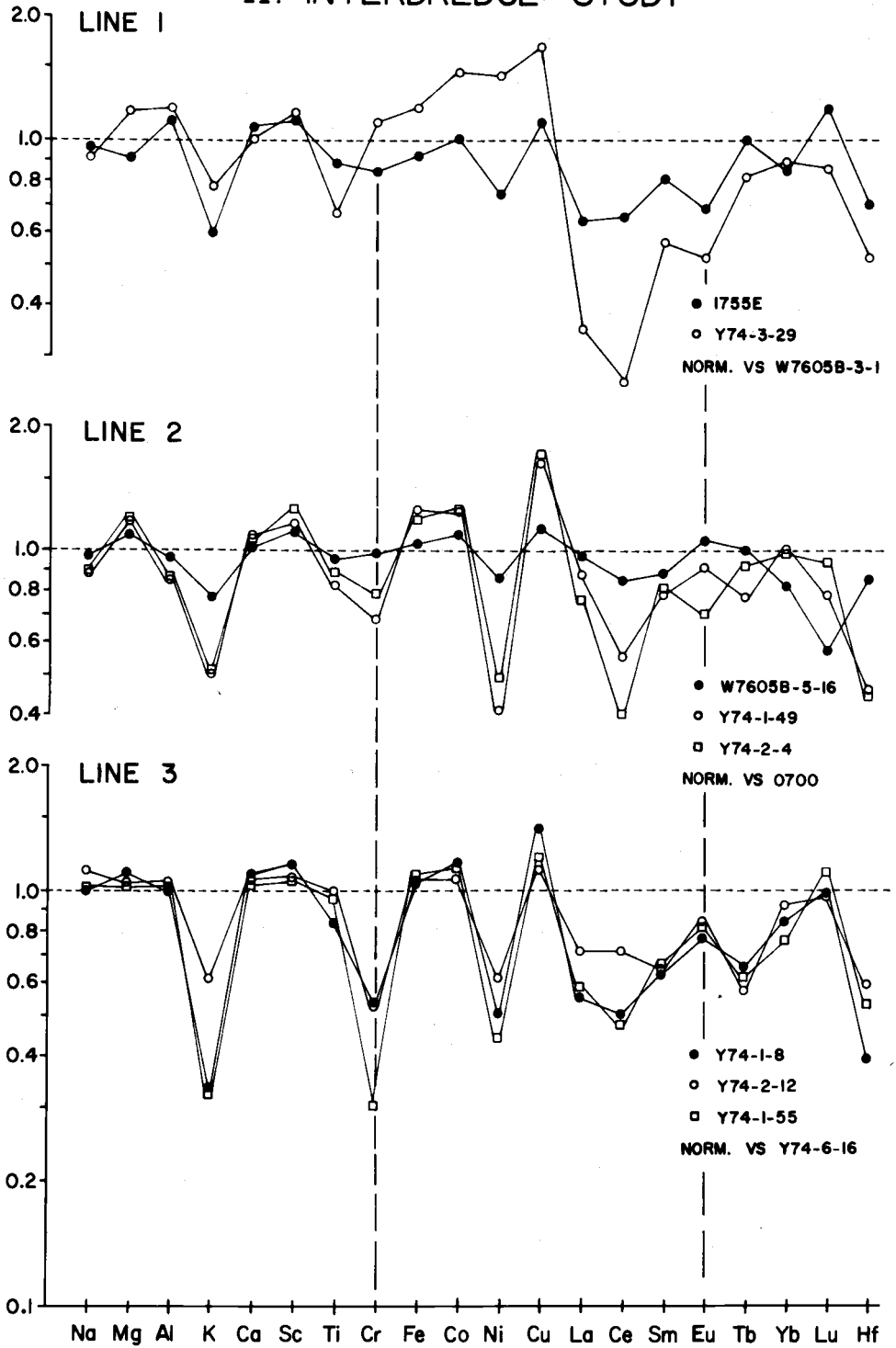


Figure 12. Normalization plots used for interdredge relationship study.

(see Figure 11). The normalization plots display consistent depletion of K, Ti, Cr, Ni, and REE accompanied by enrichment of Ca, Sc, Fe, Co and Cu toward Factor 3. This occurs in all cases used in the normalization plots, with the exception of Y74-3-29 which was strongly enriched in Cr and Ni, as reflected by the appearance of Cr-rich spinel and olivine phenocrysts (Figure 9). These patterns are dissimilar to those observed under intradredge relationship study. Gorda Ridge basalts are characterized by higher K, Cr, Ni and REE abundances than Juan de Fuca's Y74-DR1, -DR2 and -DR3.

DISCUSSION

Generally, the most important feature observed in the compositional variation study is that the REE enrichment or depletion is not closely correlated with the behavior of most major elements. This lack of correlation is also reflected in the distribution of Cr, Ni, Ti, K, Sc and Co.

If all the liquids generated beneath Juan de Fuca and Gorda Ridges are genetically related to a single homogeneous source, then any differences in composition may have developed either during partial melting episode, during fractional crystallization within the magma chamber or as the liquid ascends from the magma chamber, or during interaction with altered-wall rocks and other chemical reservoirs.

Thompson (1973) has postulated that liquids become enriched with K, H₂O, Cu and REE during interaction with altered wall-rocks. If so, reaction between magma and altered wall-rocks could account for marginal increases in these elements in the Gorda Ridge basalts. However, Thompson also pointed out that no changes in Ti and Sc contents occur during interaction and this is not consistent with the observation for Gorda Ridge basalts. I have not made detailed chemical analyses of altered basalts, although such studies, along with isotopic studies and microprobe investigations, would greatly enhance an understanding of the nature of the reaction between the

wall-rock and the liquid. In the meantime, I will focus on chemical differences that must be a result of partial melting and fractional crystallization processes.

Theoretical Introduction to Fractional Crystallization Models

The behavior of a dispersed element between coexisting solid phases in silicate melts can be described in terms of a Nernst partition coefficient (D_E) (modified from Gast, 1968):

$$D_E = \frac{C_E^{\text{crystal}}}{C_E^{\text{liquid}}}$$

where C_E^{crystal} = concentration of the element E in the crystalline phase, C_E^{liquid} = concentration of the element in the liquid phase; where more than one crystalline phase is involved

$$D = \sum_i X_i D_i$$

where X_i 's are the weight fractions of different minerals ($\sum_i X_i = 1$) and the D 's are the partition coefficients of the element for those minerals.

Two limiting fractionation processes have been recognized. The situation where the total solid phase is in equilibrium with the coexisting liquid phases is denoted as bulk equilibrium, whereas the situation where crystals are removed from contact with the liquid

(as in the case of zoned crystals) soon after their formation is denoted as surface equilibrium (Albarede and Bottinga, 1972).

Under bulk equilibrium conditions, the concentration of an element in the liquid (L) and solid (S) is obtained from the equations:

$$\frac{C_L}{C_O} = \frac{1}{F + D(1-F)} \quad \text{and} \quad \frac{C_S}{C_O} = \frac{D}{F + D(1-F)}$$

where C_L = concentration of the element in the aggregate liquid;

C_O = initial concentration of the element in the liquid;

F = fraction of original liquid remaining;

D = bulk partition coefficient;

C_S = concentration of the element in the bulk residual solid.

Similarly, under surface equilibrium conditions:

$$\frac{C_L}{C_O} = F^{(D-1)} \quad \text{and} \quad \frac{C_S}{C_O} = \frac{(1-F)^D}{1-F}$$

There is considerable experimental data showing that the partition coefficients vary as a function of temperature, pressure, oxygen fugacity, etc. (Sun et al., 1974; Leeman, 1974; Grutzeck et al., 1974; Leeman and Scheidegger, 1976). Experimental determination of the liquidus temperatures of Mid-Atlantic Ridge basalts and calculations of the temperatures based on glassy matrix's $Mg^{+2}/Mg^{+2} + Fe^{+2}$ ratio and olivine composition (Frey et al., 1974) suggest that the temperature of the partial melting event is likely to be $\sim 1300^\circ C$.

In addition, experimental studies by Sun et al. (1974) indicated that plagioclase and groundmass of Gorda Ridge sample #1154 (first analyzed by Kay et al., 1970) were last in equilibrium at 1194°C and at calculated oxygen fugacity of $10^{-8.76}$ atm. Hence, the partition coefficients used for partial melting models and for fractional crystallization models are calculated wherever available based on temperatures at 1300°C and 1200°C, respectively. These values are listed in Tables 3 and 4.

Testing of Fractional Crystallization Models against Relative Trace Element Data

Employing the partition coefficients of different minerals (Table 3), I attempted to simulate the relative trace element content of some fractionated liquids. Frequent occurrence of zoned crystals in Juan de Fuca and Gorda Ridge basalts (see petrographic analysis in Appendix D) suggests that surface equilibrium model is probably a more realistic approximation to condition of volcanic rocks. Thus all of the trace element contents are calculated according to the surface equilibrium model.

Figure 13 shows the relationship between the liquids produced by varying proportion of mineral phases removed. Each plot illustrates the effect of fractionation of a single phase. The following generalization can be made from such modeling:

Table 3. Partition Coefficients Used for Fractional Crystallization Model.

| ELEMENT | OLIVINE | PLAGIOCLASE | CLINOPYROXENE |
|---------|---------|-------------|---------------|
| La | .01 | .19 | .10 |
| Sm | .01 | .07 | .50 |
| Eu | .01 | .25 | .51 |
| Yb | .02 | .04 | .62 |
| Lu | .03 | .04 | .56 |
| Hf | .01 | .04 | .60 |
| Sc | .15 | .01 | 2.00 |
| Cr | 3.00 | .01 | 7.50 |
| Ni | 16.00 | .01 | 1.80 |
| Co | 3.00 | .01 | 1.70 |

References:

OL: REE (Leeman, 1976); Sc, Cr, Ni, Ci (Leeman and Scheidegger, 1977)

PL: (Leeman, 1976)

CPX: (Arth and Hanson, 1975; Drake and Weill, 1975; Dale and Henderson, 1969)

Table 4. Partition Coefficients Used in Partial Melt Model.

| | OL | OPX | CPX | SPIN | PLAG |
|----|--------|-------|--------|--------|-------|
| La | 0.007 | 0.005 | 0.069 | 0.030 | 0.140 |
| Sm | 0.007 | 0.013 | 0.260 | 0.053 | 0.070 |
| Eu | 0.007 | 0.014 | 0.308 | 0.055 | 0.135 |
| Yb | 0.014 | 0.056 | 0.290 | 0.111 | 0.030 |
| Lu | 0.016 | 0.068 | 0.280 | 0.091 | 0.030 |
| Sc | 0.150 | 0.700 | 1.600 | 2.000 | 0.010 |
| Cr | 1.000 | 2.000 | 10.000 | 10.000 | 0.010 |
| Ni | 14.000 | 3.800 | 2.600 | 5.000 | 0.010 |
| Co | 3.500 | 1.400 | 0.720 | 2.000 | 0.010 |

References:

- OL: REE (Arth and Hanson, 1975); Sc, Cr, Co (Leeman and Scheidegger, 1977)
- OPX: (McKay and Weill, 1976); Sc, Cr, Ni, Co (Mercy and O'Hara, 1967)
- CPX: (Grutzeck et al., 1974); Eu (Sun et al., 1974); Sc, Cr (Leeman, 1976); Ni, Co (Lindstrom and Weill, 1974)
- SPIN: (Kay and Gast, 1973); Sc, Cr, Ni, Co (Leeman, 1976)
- PLAG: (Arth and Hanson, 1975); Eu (Sun et al., 1974); Sc, Cr, Ni Co (Leeman, 1976)
-

FRACTIONAL CRYSTALLIZATION MODEL

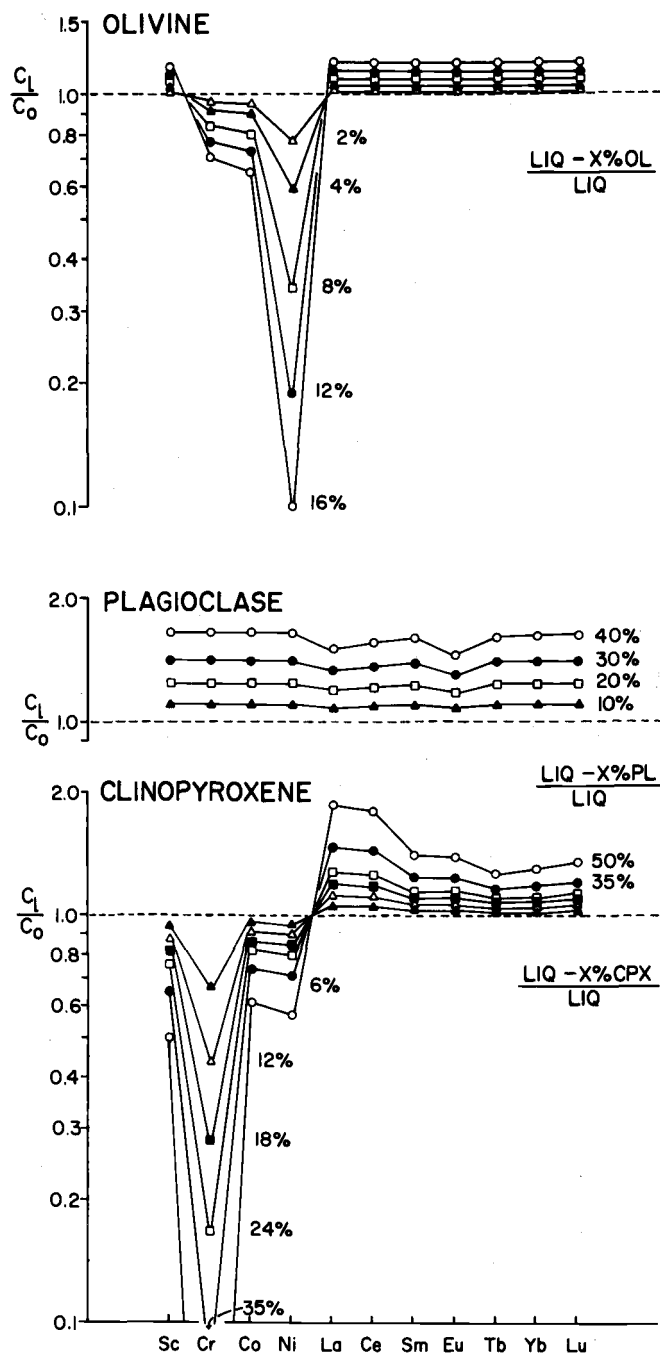


Figure 13. Effect of fractional crystallization which involves removal of X% of mineral phase from the initial liquid (LIQ).

1. Removal of olivine from the parent liquid depletes Cr, Co and Ni but enriches Sc and total REE in the fractionated liquid.

2. Removal of plagioclase enriches all the trace elements and the REE in the fractionated liquid. Plagioclase rejects Eu less strongly than other phases from the liquid, as illustrated by a negative Eu anomaly in the REE profile.

3. Removal of clinopyroxene depletes Cr and to a lesser extent Sc, Co and Ni. Although it also enriches the total REE, clinopyroxene is the only phase that depletes Sc and fractionates light REE (La and Ce) relative to the heavy REE.

Under the perhaps unlikely conditions that all the parameters (D_E values, amounts of mineral fraction removed, etc.) are valid, the calculated plots for enrichment and depletion of trace element contents derived from its parental magma should correlate closely the observed plots for enrichment and depletion of the elements illustrated in Figures 14 and 15. The observed profiles are simplified version taken from a few selections from the normalization plots shown in Figures 10 and 12. However, because of uncertainties in all parameters in addition to the analytical errors of the trace element data, some degree of deviation is expected between the observed and calculated plots.

Examination of the plots for possible correlations results in the following conclusions:

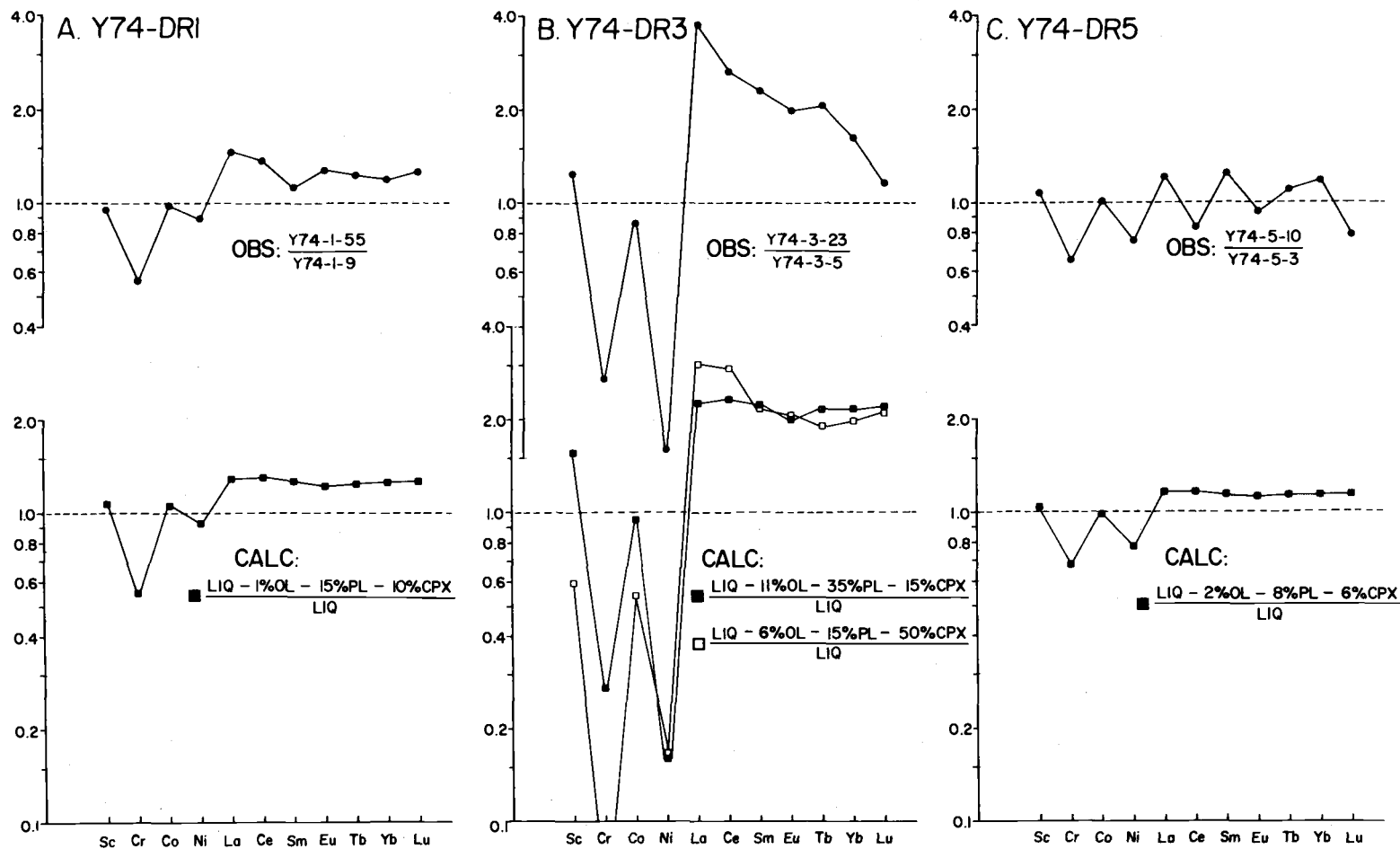


Figure 14a. Correlation between the observed intradredge normalization plots and the calculated fractional crystallization models. Plot B illustrates some difficulties in explaining the chemical variation solely by fractional crystallization.

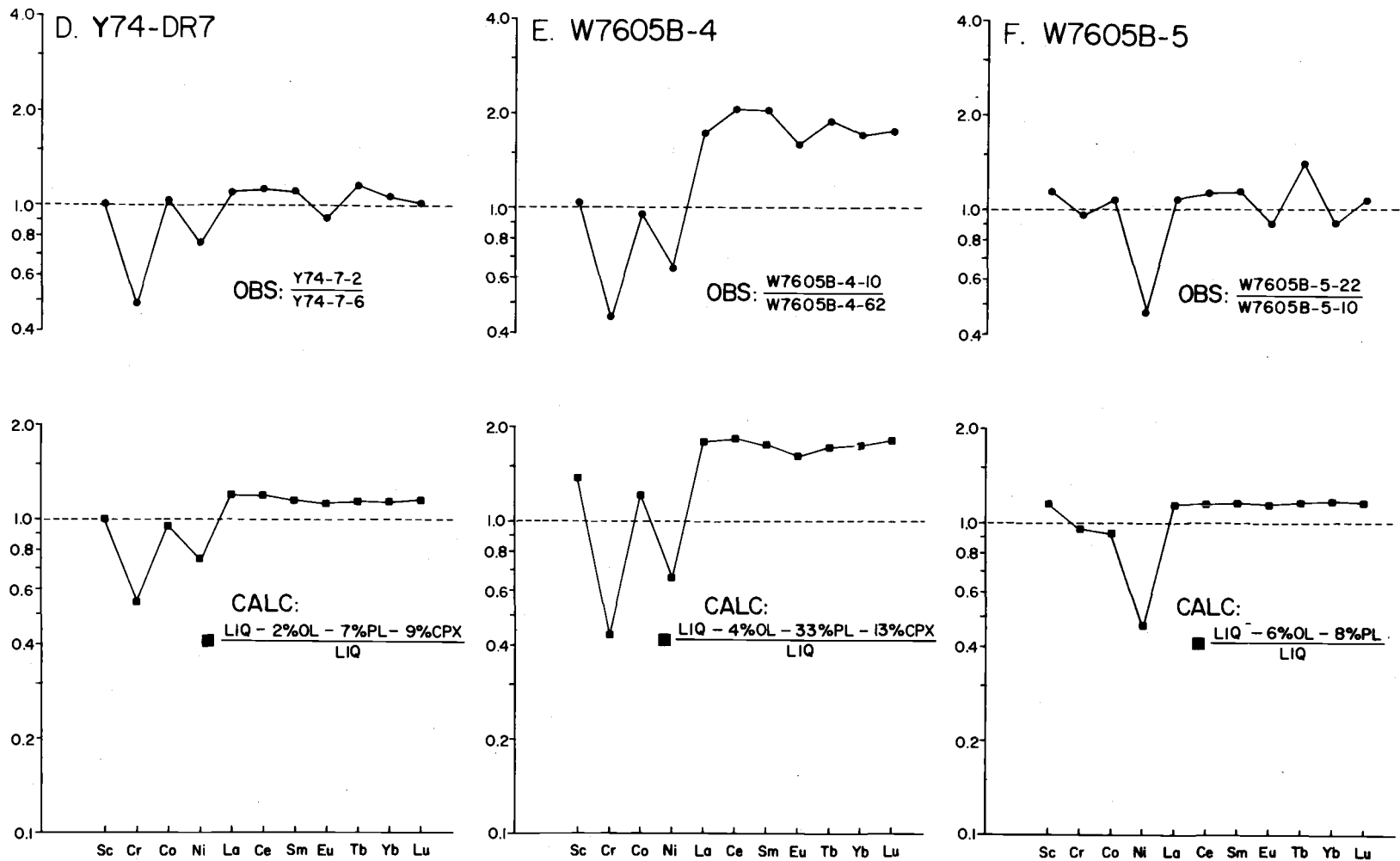


Figure 14b. Correlation between the observed intradredge normalization plots and the calculated fractional crystallization models.

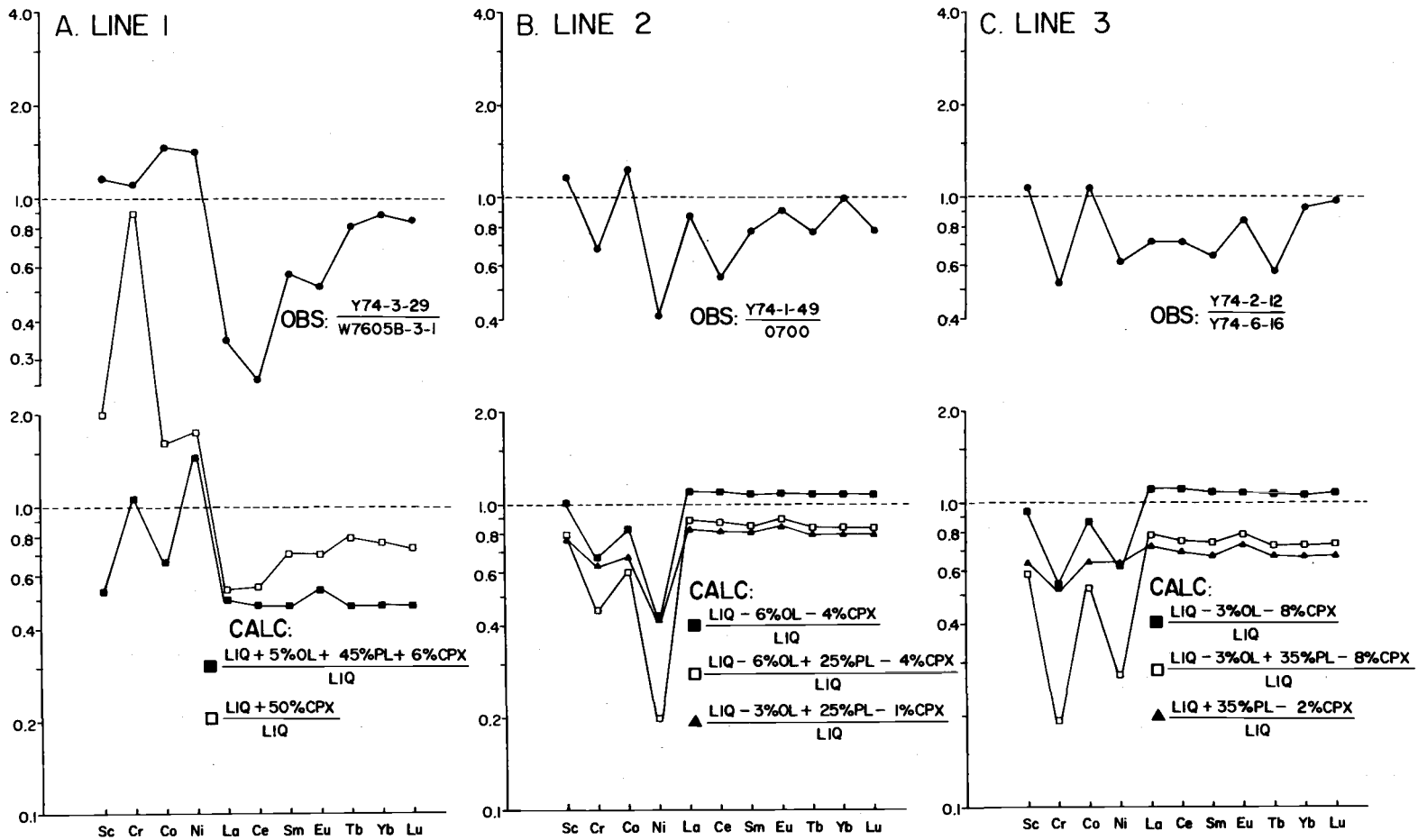


Figure 15. Correlation between the observed interdredge normalization plots and the calculated fractional crystallization models. None of the chemical variation could be well explained by fractional crystallization alone. Partial melting models appear to explain the chemical variation more clearly, as readily shown in Figure 17.

1. Figure 14 which contains normalization plots for intradredge study illustrates how enrichment in REE and depletion in Cr and Ni within each dredge haul could be explained by fractionation of plagioclase, olivine and/or clinopyroxene. Thus, each dredge haul that displays elongated field in the factor analysis may be defined by an individual crystal fractionation sequence.

2. Juan de Fuca Ridge basalts (ie. plots A, C and D in Figure 14) are characterized by marked depletion of Cr relative to Ni and REE, suggesting that clinopyroxene is an important fractionating phase in Juan de Fuca Ridge basalts. Thus, samples that cluster closer to Factor 1 apex could represent advanced stage fractionation process. Gorda Ridge basalts (ie. plots E and F) show strong depletion in Ni and in some cases strong enrichment in total REE. However, there is little significant Cr depletion in Gorda Ridge basalts as compared to Juan de Fuca Ridge basalts. This reflects only olivine and plagioclase as fractionating phases with minor clinopyroxene in some cases.

3. Positive Eu anomalies in Juan de Fuca's dredge hauls Y74-DR1, -DR2, -DR3, -DR4 and Y7305A (ie. plot A; see also Figure 10 for more evidence) could not be explained by the plagioclase fractional crystallization model.

4. Strong light REE enrichment relative to heavy REE observed in sample Y74-3-23 (plot B) demonstrates that this sample cannot be

genetically related to sample Y74-3-5 solely by fractional crystallization. The observed enrichment of La relative to the heavy REE requires a removal of more than 50% clinopyroxene which would result in stronger depletion of Cr than necessary for producing Y74-3-23.

5. Comparison of observed and calculated plots used for inter-dredge study (Figure 15) shows that depletion of total REE, K, Ti, Cr and Ni accompanied by enrichment of Sc and Co cannot be explained solely by fractional crystallization. Any attempt to match the REE profile (ie. by adding large volume of plagioclase to the initial liquid) results in erroneous patterns for the transition metals. Instead, as discussed in the following section, lower abundances of K, Ti and REE for Juan de Fuca Ridge basalts could arise as a result of larger degree of partial melting than Gorda Ridge basalts.

Theoretical Introduction to Partial Melting Models

Recent experimental work by Mysen and Kushiro (1976) shows that in at least some cases there may be little change in major element concentration of the melt over a relatively large range of melting of peridotite. This variable degree of partial melting should be particularly efficient in producing variations of REE and also K, P and Ti which are excluded from most mantle phases (Gast, 1968) without greatly affecting the major elements.

I assume that partial melting occurs as a process in which the melt remains in chemical equilibrium with the mantle residual minerals which melt in non-modal proportion. This case seems more realistic and also lends itself to a straight forward mathematical treatment based upon the non-modal batch melting equation of Shaw (1970):

$$\frac{C_L}{C_O} = \frac{1}{D + F(1-P)}$$

where P is a bulk distribution coefficient that is weighted according to the proportion (p_i) in which mantle phases melt ($P = \sum_i p_i D_i$), F is the weight fraction of melt formed and all other symbols are defined as before.

The melting proportions are taken from Schilling (1975) for two possible candidates as primary mantle source, lherzolite and feldspar peridotite. Schilling, however, was unable to discriminate the two mantle sources based only on REE study; therefore, it remains questionable which of the two model mantle sources is favorable. In this view, I intend to evaluate partial melting models in terms of two separate mantle sources.

Testing of Partial Melting Models Against Relative Trace Element Data

Employing the partition coefficients of different minerals

(Table 4) plus primary mantle assemblages and eutectic compositions provided by Schilling (1975), I attempted to simulate the relative trace element content of various partial melts, illustrated in Figure 16. The following generalization can be made from such modeling:

1. Any increase in the degree of partial melting of the lherzolite mantle source results in an enrichment of all transition metals and a depletion in total REE in the melt. A difference of 20% or more in partial melting results in stronger depletion of light REE as compared to the heavy REE.

2. Any increase in the degree of partial melting of the feldspar peridotite mantle source results in an enrichment of only Cr and Ni and a depletion in Sc, Co and the REE. A relative increase in melting controls not only the light REE depletion but also the positive Eu anomaly, as illustrated in Figure 16 (B).

Comparison of these partial melting models with the interdredge plots (Figure 17) for possible correlations results in the following conclusions:

1. It is difficult to determine which one of the two candidates for primary mantle source is favorable for two reasons. First, the observed interdredge plots show poor correlation with either the lherzolite or the plagioclase peridotite model when explained by partial melting alone. Second, to improve the correlation, particularly of the transition metals, it is necessary to invoke fractional

PARTIAL MELTING MODELS

A: LHERZOLITE MODEL

from Schilling (1975)

| | OL | OPX | CPX |
|---------------------|-----|-----|-----|
| Primary Assemblage: | .60 | .25 | .15 |
| Melting Proportion: | .25 | .20 | .55 |

27% melt, CPX depleted

B: PLAG-PERIDOTITE MODEL

from Schilling (1975)

| | OL | OPX | CPX | PL |
|---------------------|-----|-----|-----|-----|
| Primary Assemblage: | .51 | .17 | .17 | .15 |
| Melting Proportion: | .11 | .11 | .28 | .50 |

30% melt, PL depleted

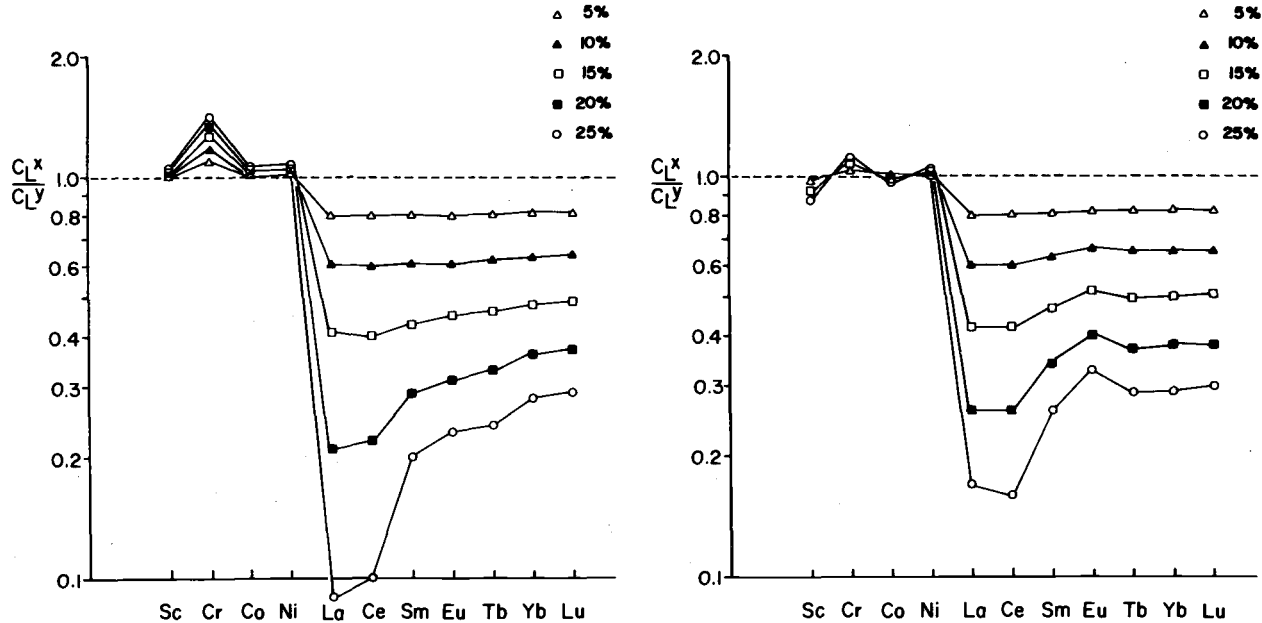


Figure 16. Effect of partial melting. Each line shows the effect of different proportion of melting (on relative scale of %). C_L^x = concentration of the element in the liquid that is derived by x degree of partial melting ($x = 25\%$). C_L^y = concentration of the element in the liquid that is derived by y degree of partial melting ($y = 20, 15, 10, 5$ and 1%).

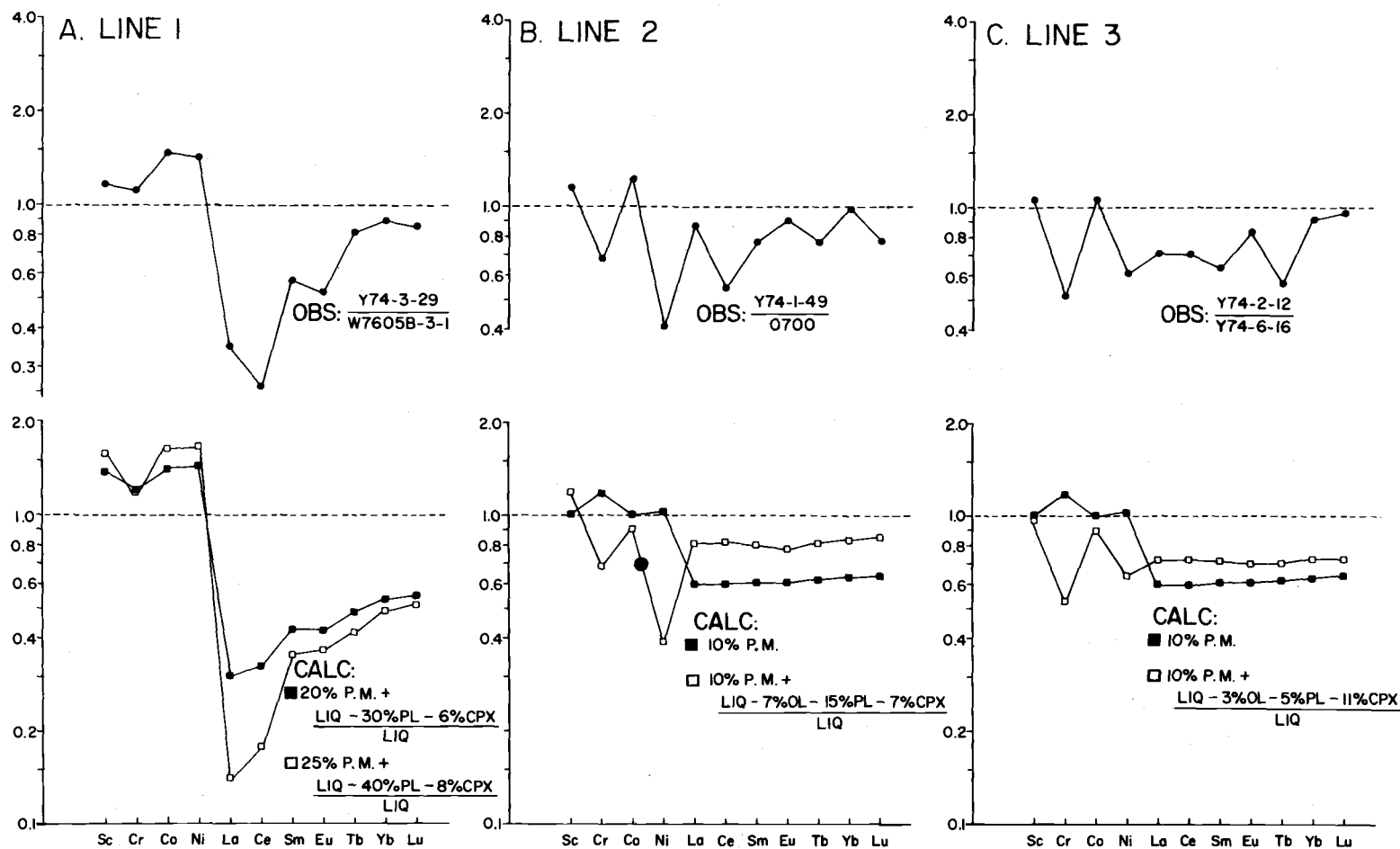


Figure 17. Correlation between the observed interdredge normalization plots and the calculated partial melting model. Plots B and C are examples of an improvement in the profile after fractional crystallization model is superimposed upon the partial melting model.

crystallization upon the partial melting model (see plots B and C, Figure 17). In this way, fractional crystallization will perturb the pattern and therefore obliterate the possibility for distinguishing between partial melting equilibration with a spinel or plagioclase peridotite mantle. However, the fact that spinel phenocrysts occur in some picritic samples and are thought to have equilibrated with the mantle residue at the time of partial melting (Frey et al., 1974) encourages the possibility of using spinel peridotite as the favorable candidate. Furthermore, extreme depletion of light REE in the picritic samples (this is readily seen in plot A, Figure 17) correlates best with the calculated model based on spinel peridotite source.

2. The fact that each plot of the observed data correlates better with the calculated partial melting model than with the calculated fractional crystallization model alone (compare Figure 17 with Figure 15) supports the contention that Juan de Fuca Ridge basalts (particularly Y74-DR1, -DR2 and -DR3) are derived by a larger degree of partial melting than are Gorda Ridge basalts, on a relative scale of 10% difference in degree of partial melting. In addition, lower abundances of K and Ti in Juan de Fuca Ridge basalts agree with Gast's (1968) contention that increasing partial melting reduces the K and Ti contents in the melts. Furthermore, dredge hauls that cluster close to Factor 3 apex as seen in factor analysis (Figure 7)

could represent larger degrees of partial melting as compared to dredge hauls that gather along Factors 1 and 2.

3. Positive Eu anomalies in Juan de Fuca's dredge hauls Y74-DR1, -DR2, -DR4 and Y7305A accompanied by enrichment of Ca, Sc and Co (see Figure 12 and plots B and C, Figure 17) could reflect derivation of these liquids by partial melting of plagioclase peridotite. However, a 10% Eu enrichment would require more than 25% difference in the degree of partial melting which in turn depletes the total REE more than necessary to fit the observed profile (compare Figure 17 with Figure 16). I postulate that positive Eu anomaly accompanied by Ca enrichment in these liquids arose as a result of melting and mixing of plagioclase peridotite into the rising lherzolite diapir. This suggests that liquids that were derived from larger degrees of partial melting from the lherzolite mantle must have risen as diapirs from depth, entered the stability field of plagioclase peridotite during ascent (Herzberg, 1972) and subsequently remelted a portion of PL-peridotite as the liquid is convected back into deeper hotter portion of the magma chamber (ie. resorption caused by increasing temperature at constant pressure: Melson and Thomsson, 1971).

4. Juan de Fuca's picritic samples Y74-3-5, 3-13, and 3-29 (ie. plot A, Figure 17), which show unusually strong depletion in light REE relative to heavy REE, require more than 25% difference

in degree of melting to produce the observed light REE/heavy REE ratio. However, all of the phases that melt have REE partition coefficients less than unity, thus 25% or more difference in melting will produce overall depletion of REE as well as fractionating the light and heavy REE. All of these considerations are consistent with, if not supportive of, the interpretation that these picritic samples are not related by partial melting. The extent of light REE depletion for these picritic samples is far too pronounced for its possible derivation from the same mantle source as the other normal ridge basalts.

Schilling (1975) attempted to explain the origin of picritic basalts from DSDP Leg 3, which also showed anomalously depleted light REE, by postulating that an unusual history of repeated basalt extraction has occurred in the low-velocity layer. It was suggested that rift-shifting could retap a volume of the upper asthenosphere that had previously been a source of basaltic magma so that a more light REE depleted liquid would be produced during the subsequent removal of magma.

In addition, not all picritic and OL-rich tholeiites are anomalously light REE depleted. Basalts of this kind that were collected from the FAMOUS area reveal light REE enrichment relative to the heavy REE, because of its association with the "transition" zone (Schilling, 1975; White and Bryan, 1977). Regardless of the similarities and contrasts in major element chemistry and mineralogy, the differences

in REE profiles could be attributed to some variations in the mantle.

Compositional variations in ocean ridge basalts have also been attributed to different P-T (depths) conditions. Experimental data of Green and Ringwood (1967) suggest that undersaturated high-Al (probably OL-rich and picritic) magmas form by relatively small degrees of partial melting at depths of 25-30 km. in equilibrium with Al-poor pyroxenes. Bass (1971) and Scheidegger (1973) concluded that these basalts are generated at greater depths than what is normally proposed for quartz-normative and hypersthene-normative magmas (15 km). The occurrence of Juan de Fuca's picritic samples could reflect larger degree of partial melting (and less low P modifications) at greater depths than other basalts in Juan de Fuca and Gorda Ridges, and this would generate basalts with much greater light REE depletion.

CONCLUSIONS

A detailed investigation of the chemical variations in mid-ocean ridge basalts reveals that Juan de Fuca Ridge basalts have undergone more extensive fractional crystallization than Gorda Ridge basalts. Most of the Gorda Ridge basalts appear to be modified by low-P fractional crystallization processes involving the removal of olivine and plagioclase phases. In southern Juan de Fuca Ridge area, however, subsequent crystallization results in an increase of pyroxene components in the residual liquids, leading to high level fractional crystallization of clinopyroxene in addition to olivine and plagioclase. Marked enrichment of Fe and Ti, accompanied by successive enrichment of total REE and depletion of Cr and Ni takes place in the southern Juan de Fuca Ridge, as a result of this high-level fractional crystallization process. This conclusion is in accordance with the "magnetic telechemistry" hypothesis of Vogt and Byerly (1976) who suggested that Fe-Ti enrichment is result of late-stage crystallization processes and is not characteristic of a plume-derived source.

North of high Fe-Ti region, Juan de Fuca's dredge hauls Y74-DR1, -DR2, -DR3, and -DR4 display lower abundances of K, Ti and light REE prior to the onset of fractional crystallization suggesting that these liquids were initially derived by a larger degree of melt. The picritic samples (Y74-3-5, 3-13, and 3-29) could arise from an

even larger degree of melting followed by lesser low-pressure modification. They also occur in an area of low magnetic amplitude noted by Vogt and Byerly (1976). The similarity in low K and Ti contents between the picritic samples and the high Mg-Ca basalts of the Sovanco Fracture Zone reported by Barr and Chase (1974) (see Figure 1) suggests that areas of low magnetic amplitudes could reflect larger degrees of partial melting. This is yet to be tested with REE and transition metals not reported by Barr and Chase (1974). Further tests on partial melting models could also be made by analyzing for Pb (Church and Tatsumoto, 1975), Sr (Gast, 1968; Kay et al., 1970; Hedge and Peterman, 1970), and Nd isotopes (DePaolo and Wasserburg, 1976; Richard et al., 1976). Fractionation in these elements are known to be sensitive indicators of fractionation in K and the light REE. The cause of strong light REE and K depletions in the source may then be confirmed by these isotopic analyses.

It is speculated that spreading centers that produce picritic basalts (ie. central and northernmost parts of Juan de Fuca Ridge) overlies some localized diapiric intrusions. This type of basalt may be related to some breaking-up and microfracturing of the spreading center during reorientation, so that rifting could tap a deep magma source formed by a large degree of partial melting. Then eruption would take place that allows little time for fractional crystallization

to occur, thus giving rise to random, more primitive basalts.

In contrast, areas that produce well differentiated basalts (ie. Gorda Ridge and southern Juan de Fuca Ridge) probably overlie more permanent magma chambers, which contain cooler and more differentiated lava. The extent of fractional crystallization may then be reflected by the degree of permanence of these magma chambers. Juan de Fuca's high Fe-Ti basalts would then have come from a more permanent source as a result of a longer crystallization history. And Gorda Ridge's differentiated basalts would come from an even less permanent source, thus leading to less low-pressure modifications as compared to Juan de Fuca Ridge basalts.

BIBLIOGRAPHY

- Albarede, F., and Bottinga, Y., 1972, Kinetic disequilibrium in trace element partitioning between phenocrysts and host lava, *Geochim. Cosmochim. Acta*, 36, 141-156.
- Arth, J. G., and Hanson, G. N., 1975, Geochemistry and origin of the early precambrian crust of northeastern Minnesota, *Geochim. Cosmochim. Acta*, 39, 325-362.
- Barr, S. M., 1974, Seamount chains formed near the crest of Juan de Fuca Ridge, Northeast Pacific Ocean, *Mar. Geol.*, 17, 1-19.
- Barr, S. M., and Chase, R. L., 1974, Geology of the northern end of Juan de Fuca Ridge and sea-floor spreading, *Can. J. Earth Sci.*, 11, 1384-1406.
- Bass, M. N., 1971, Variable abyssal basalt populations and their relation to sea-floor spreading rates, *Earth Planet. Sci. Lett.*, 11, 18-22.
- Blakely, R. J., 1974, Geomagnetic reversals and crustal spreading rates during the Miocene, *J. Geophys. Res.*, 79, 2979-2985.
- Bryan, W. B., and Moore, J. G., 1977, Compositional variations of young basalts in the mid-Atlantic Ridge rift valley near lat. 36°49'N, *Geol. Soc. Amer. Bull.*, 88, 556-570.
- Bryan, W. B., 1972, Morphology of quench crystals in submarine basalts, *J. Geophys. Res.*, 77 (29), 5812.
- Bryan, W. B., et al., 1976, Inferred geologic settings and differentiation in basalts from the deep-sea drilling project, *J. Geophys. Res.*, 81 (23), 4285-4304.
- Carmichael, I. S. E., Turner, F. J., and Verhoogen, J., 1974, *Igneous Petrology*: McGraw-Hill, New York, 739 p.
- Church, S. E., and Tatsumoto, M., 1975, Lead isotope relations in oceanic ridge basalts from the Juan de Fuca-Gorda Ridge area, N. E. Pacific Ocean, *Contrib. Mineral. Petrol.*, 53, 253-279.

- Clague, D. A., and Bunch, T. E., 1976, Formation of ferrobasalt at east Pacific mid-ocean spreading centers, *J. Geophys. Res.*, 81 (23), 4247-4256.
- Corliss, J. B., 1970, Mid-ocean ridge basalts, Ph.D. thesis, University of California at San Diego, La Jolla.
- Dale, I. M., and Henderson, P., 1972, The partition of transition elements in phenocryst-bearing basalts and the implications about melt structure, 24th Internat. Geolog. Cong. Sec. 10, 105-111.
- Dehlinger, P., R. W. Couch, D. A. McManus, and M. Gemperle, 1971. Northeast Pacific structure, *The Sea*, Vol. 4, Part II: 133-189 (John Wiley and Sons, Inc.).
- DePaolo, D. J., and Wasserburg, G. J., 1976, Nd isotopic variations and petrogenetic models, *Geophys. Res. Lett.*, 3 (5), 249-252.
- Detrick, R. S., and Lynn, W. S., 1975, The origin of high-amplitude magnetic anomalies at the intersection of the Juan de Fuca Ridge and Blanco Fracture Zone, *Earth Planet. Sci. Lett.*, 26, 105-113.
- Elvers, D., et al., 1973, Asymmetric spreading across the Juan de Fuca and Gorda Rises as obtained from a detailed magnetic survey, *Earth Planet. Sci. Lett.*, 20, 211-219.
- Frey, F. A., Bryan, W. B., and Thompson, G., 1974, Atlantic Ocean floor: Geochemistry and petrology of basalts from legs 2 and 3 of the Deep-Sea Drilling Project, *J. Geophys. Res.*, 79 (35), 5507-5527.
- Fukui, S., 1976, Laboratory techniques used for atomic absorption spectrophotometric analysis of geologic samples, Oregon State University, School of Oceanography Reference 76-10.
- Gast, P. W., 1968, Trace element fractionation and the origin of tholeiitic and alkaline magma types, *Geochim. Cosmochim. Acta*, 32, 369-396.
- Green, D. H., and Ringwood, A. E., 1967, The genesis of basaltic magmas, *Contrib. Mineral. Petrol.*, 15, 103-190.

- Grutzeck, M., Kridelbaugh, S., and Weill, D., 1974, The distribution of Sr and REE between diopside and silicate liquid, *Geophys. Res. Lett.*, 1 (6), 273-275.
- Handschumacher, D. W., 1976, Post Eocene plate tectonics of the Eastern Pacific, in Sutton, G. H., et al., eds., *The Geophysics of the Pacific Ocean Basin and its margin: The Woollard Volume*: Amer. Geophys. Union, Washington, D. C.
- Haskin, L. A., et al., 1967, Relative and absolute terrestrial abundances of the rare earths, presented at Symposium on origin and distribution of the elements, 1st meeting of the International Association of Geochemistry and Cosmochemistry, Paris, May 8-11, 1967.
- Hedge, C. E., and Peterman, Z. E., 1970, The strontium isotope composition of basalts from the Gorda and Juan de Fuca Rises, Northeastern Pacific Ocean, *Contrib. Mineral. Petrol.*, 27, 114-120.
- Imbrie, J., and Kipp, N. G., 1971, A new micro-paleontological method of quantitative paleoclimatology: Application to a late Pleistocene Caribbean core, in Turekian, K. K., ed., *The late Cenozoic glacial ages*: New Haven, Yale Univ. Press, 71-181.
- Irvine, T. N., 1967, Chromian spinel as a petrogenetic indicator, *Can. J. Earth Sci.*, 4, 71-103.
- Kay, R. W., and Gast, P. W., 1973, The rare earth content and origin of alkali rich basalts, *Jour. Geology*, 81, 653-682.
- Kay, R. W., Hubbard, M. J., and Gast, P., 1970, Chemical characteristics and origins of oceanic ridge volcanic rocks, *J. Geophys. Res.*, 75, 1585-1613.
- Leeman, W. P., 1974, Petrogenesis of McKinney (Snake River) olivine tholeiite in light of rare-earth element and Cr/Ni distributions, *Geol. Soc. Amer. Bull.*, 87, 1582-1586.
- Leeman, W. P., and Scheidegger, K. F., 1977, Olivine/liquid distribution coefficients and a test for crystal-liquid equilibrium, *Earth Planet. Sci. Lett.*, 35 (2), 247-257.

- Lindstrom, D. J., and Weill, D. F., 1974, Distribution of transition metal ions between diopside and coexisting liquid in the system diopside-albite-anorthite, EOS Trans. (AGU), 55, 473.
- Lister, C. R. B., 1969, Preliminary heat-flow profile across the Juan de Fuca Ridge; interpretation of a high value (abstr): EOS (Amer. Geophys. Union, Trans.), 50 (1), 633.
- _____, 1970, A heat-flow profile across the Juan de Fuca Ridge near 47° (Abstr.): EOS (Amer. Geophys. Union, Trans.), 51 (4), 317.
- _____, 1971, Crustal magnetization and sedimentation near two small seamounts west of the Juan de Fuca Ridge, northeast Pacific; J. Geophys. Res., 76 (20), 4824-4841.
- Melson, W. G., and Thompson, G., 1970, Petrology of a transform fault zone and adjacent ridge segments, Phil. Trans. Roy. Soc. London A, 268, 423-441.
- Mercy, E., and O'Hara, M. J., 1967, Distribution of Mn, Cr, Ti and Ni in co-existing minerals of ultramafic rocks, Geochim. Cosmochim. Acta, 31, 2331-2341.
- Miyashiro, A., Shido, F., and Ewing, M., 1969, Diversity and origin of abyssal tholeiite from the Mid-Atlantic Ridge near 24° and 30° North latitude, Contrib. Mineral. Petrol., 23, 38-52.
- _____, 1970, Crystallization and differentiation in abyssal tholeiites and gabbros from mid-oceanic ridges, Earth Planet. Sci. Lett., 7, 361-365.
- Moore, J. G., 1970, Water content of basalt erupted on the ocean floor, Contrib. Mineral. Petrol., 272-279.
- Morgan, W. J., 1972, Deep mantle convection plumes and plate motions, Amer. Assoc. Pet. Geol. Bull., 56, 203-213.
- Murali, A. V., Leeman, W. P., et al., 1976, Evaluation of fractionation and hybridization models for Kilauea eruptions and probable mantle source of Kilauea and Mauna Loa tholeiitic basalts, Hawaii, Jour. Petrol., in press.
- Mysen, B. O., and Kushiro, I., 1976, Melting behavior of peridotite at high pressure, EOS Trans. (AGU), 57, 354.

- Philpotts, J. A., Schnetzler, C. C., and Hart, S. R., 1969, Submarine basalts: some K, Rb, Sr, Ba, Rare-earth, H₂O and CO₂ data bearing on their alteration, modification by plagioclase, and possible source materials, *Earth Planet. Sci. Lett.*, 7, 293-299.
- Richard, P., Shimizu, N., and Allegre, C. J., 1976, ¹⁴³Nd/¹⁴⁶Nd, A natural tracer: an application to oceanic basalts, *Earth Planet. Sci. Lett.*, 31, 269-278.
- Scheidegger, K. F., 1973, Temperatures and compositions of magmas ascending along mid-ocean ridges, *J. Geophys. Res.*, 78 (17), 3340-3355.
- Schilling, J. -G., 1971, Sea-floor evolution: Rare-earth evidence, *Phil. Trans. Roy. Soc. London A*, 268, 663-706.
- _____, 1973a, Afar mantle plume: Rare-earth evidence, *Nature Phys. Sci.*, 242, 2-5.
- _____, 1973b, Iceland mantle plume: Geochemical study of Reykjanes Ridge, *Nature*, 242, 565-571.
- _____, 1975a, Rare-earth variations across "normal segments" of the Reykjanes Ridge, 60°-53°N, Mid-Atlantic Ridge, 29°S, and evidence on the composition of the underlying low-velocity layer, *J. Geophys. Res.*, 80 (11), 1459-1473.
- _____, 1975b, Azores mantle blob: Rare-earth evidence, *Earth Planet. Sci. Lett.*, 25, 103-115.
- Schilling, J. -G., and Bonatti, E., 1975, East Pacific Ridge (2°S-19°S) versus Nazca, intraplate volcanism: Rare-earth evidence, *Earth Planet. Sci. Lett.*, 25, 93-102.
- Shaw, D. M., 1970, Trace element fractionation during anatexis, *Geochim. Cosmochim. Acta*, 34, 237-243.
- Shido, F., Miyashiro, A., and Ewing, M., 1971, Crystallization of abyssal tholeiites, *Contrib. Mineral. Petrol.*, 31, 251-266.
- Shor, G. G., Jr., Dehlinger, P., Kirk, H. H., and French, W. S., 1968, Seismic refraction studies off Oregon and northern California, *J. Geophys. Res.*, 73 (6), 2175-2194.

- Sun, C., Williams, R. J., and Sun, S., 1974, Distribution coefficients of Eu and Sr for plagioclase-liquid and clinopyroxene-liquid equilibria in oceanic ridge basalt: an experimental study, *Geochim. Cosmochim. Acta*, 38, 1415-1433.
- Thompson, G., 1973, A geochemical study of the low temperature interaction of seawater and oceanic igneous rocks, *EOS Trans.*, (AGU), 54 (11), 1015-1018.
- Vine, F. J., 1968, Magnetic anomalies associated with mid-ocean ridges, *Nature*, 199, 947.
- Vogt, P. R., and Byerly, G. R., 1976, Magnetic anomalies and basalt composition in the Juan de Fuca-Gorda Ridge area, *Earth Planet. Sci. Lett.*, 33, 185-207.
- Vogt, P. R., and Johnson, G. L., 1973, Magnetic telechemistry, *Nature*, 245, 373.
- White, W. M., and Bryan, W. B., 1977, Sr-isotope, K, Rb, Cs, Sr, Ba, and rare-earth geochemistry of basalts from the FAMOUS area, *Geol. Soc. Amer. Bull.*, 88, 571-576.

APPENDICES

APPENDIX A. ATOMIC ABSORPTION SPECTROPHOTOMETRIC
AND INSTRUMENTAL NEUTRON ACTIVATION
ANALYSES PLUS CIPW NORMATIVE CALCULA-
TIONS FOR JUAN DE FUCA AND GORDA RIDGE
BASALTS.

All oxides are given in weight percents. FeO* signifies total Fe content in form of FeO. Sc, Cr, Ni, Co and Cu are given in weight parts per million. "---" for CIPW normative calculation signifies zero values.

JUAN DE FUCA RIDGE BASALTS

| Sample # | 1-8 | 1-9 | 1-49 | 1-55 | 2-3 | 2-4 | 2-6 |
|--------------------------------|------|-------|------|------|------|------|------|
| SiO ₂ | 49.5 | 51.5 | 50.5 | 50.2 | 50.6 | 50.4 | 50.6 |
| Al ₂ O ₃ | 14.2 | 14.4 | 14.4 | 14.5 | 14.1 | 14.5 | 13.6 |
| CaO | 12.0 | 12.1 | 12.2 | 11.5 | 11.3 | 12.1 | 12.9 |
| MgO | 7.68 | 7.69 | 7.76 | 7.18 | 7.17 | 7.79 | 7.43 |
| K ₂ O | .08 | .08 | .09 | .08 | .14 | .09 | .15 |
| Na ₂ O | 2.42 | 2.40 | 2.42 | 2.48 | 2.45 | 2.45 | 2.62 |
| FeO* | 10.6 | 10.6 | 10.3 | 11.2 | 10.2 | 9.8 | 10.3 |
| TiO ₂ | 1.46 | 1.43 | 1.36 | 1.68 | 1.90 | 1.47 | 1.73 |
| TOTAL | 98.1 | 100.3 | 99.3 | 98.9 | 98.0 | 98.9 | 99.5 |
| Sc | 46 | 45 | 43 | 43 | 43 | 47 | 44 |
| Cr | 158 | 159 | 151 | 89 | 149 | 173 | 151 |
| Ni | 41 | 40 | 44 | 36 | 43 | 53 | 47 |
| Co | 50 | 50 | 49 | 49 | 47 | 49 | 47 |
| Cu | 100 | 103 | 101 | 85 | 80 | 106 | 80 |

CIPW NORMS

| | | | | | | | |
|-----|-------|-------|-------|-------|-------|-------|-------|
| QTZ | --- | 2.41 | --- | --- | 1.52 | --- | --- |
| NE | --- | --- | --- | --- | --- | --- | --- |
| OR | .48 | .46 | .53 | .48 | .84 | .54 | .87 |
| AB | 20.76 | 19.74 | 20.51 | 21.09 | 21.04 | 20.85 | 22.15 |
| AN | 28.09 | 27.65 | 28.43 | 28.45 | 27.46 | 28.69 | 25.05 |
| DI | 25.69 | 24.31 | 25.41 | 22.84 | 23.87 | 25.02 | 31.14 |
| HY | 15.80 | 20.50 | 18.20 | 21.25 | 29.77 | 28.34 | 11.40 |
| OL | 3.98 | --- | 1.90 | .21 | --- | 1.52 | 3.77 |
| IL | 2.81 | 2.64 | 2.59 | 3.21 | 3.66 | 2.81 | 3.28 |
| MT | 1.93 | 1.85 | 1.86 | 2.01 | 1.87 | 1.78 | 1.86 |
| AP | .48 | .46 | .48 | .48 | .48 | .48 | .47 |

JUAN DE FUCA RIDGE BASALTS (CONT.)

| Sample # | 2-12 | 3-5 | 3-13 | 3-23 | 3-29 | 4-2 | 4-3 |
|--------------------------------|-------|------|-------|------|------|------|------|
| SiO ₂ | 51.4 | 48.0 | 49.7 | 50.4 | 48.1 | 49.9 | 50.5 |
| Al ₂ O ₃ | 14.7 | 17.7 | 17.2 | 14.0 | 17.5 | 13.5 | 14.3 |
| CaO | 11.5 | 11.6 | 11.6 | 11.7 | 11.7 | 11.2 | 11.5 |
| MgO | 7.35 | 9.88 | 10.05 | 6.71 | 9.60 | 6.92 | 7.70 |
| K ₂ O | .15 | .05 | .05 | .13 | .08 | .21 | .19 |
| Na ₂ O | 2.71 | 2.11 | 2.21 | 2.76 | 2.20 | 2.51 | 2.47 |
| FeO* | 10.6 | 9.5 | 9.8 | 11.0 | 9.7 | 10.7 | 10.0 |
| TiO ₂ | 1.74 | .82 | .83 | 1.74 | .82 | 2.14 | 1.69 |
| TOTAL | 100.3 | 99.8 | 101.5 | 98.5 | 99.8 | 97.2 | 98.5 |
| Sc | 43 | 37 | 39 | 46 | 40 | 41 | 41 |
| Cr | 154 | 313 | 335 | 84 | 328 | 204 | 241 |
| Ni | 49 | 223 | 220 | 35 | 216 | 54 | 70 |
| Co | 46 | 58 | 61 | 49 | 60 | 43 | 45 |
| Cu | 80 | 109 | 104 | 92 | 108 | 68 | 67 |

CIPW NORMS

| | | | | | | | |
|-----|-------|-------|-------|-------|-------|-------|-------|
| QTZ | --- | --- | --- | --- | --- | .99 | .20 |
| NE | --- | --- | --- | --- | --- | --- | --- |
| OR | .88 | .30 | .29 | .78 | .47 | 1.27 | 1.13 |
| AB | 22.73 | 17.98 | 18.33 | 23.56 | 18.56 | 21.73 | 21.09 |
| AN | 27.48 | 39.17 | 36.28 | 25.66 | 37.52 | 25.75 | 27.62 |
| DI | 23.13 | 13.93 | 15.01 | 26.09 | 15.28 | 24.54 | 23.59 |
| HY | 19.53 | 6.71 | 13.99 | 17.09 | 8.64 | 19.13 | 20.84 |
| OL | 0.65 | 17.98 | 12.20 | 1.04 | 15.60 | --- | --- |
| IL | 3.28 | 1.76 | 1.73 | 3.33 | 1.74 | 4.16 | 3.24 |
| MT | 1.88 | 1.71 | 1.72 | 1.99 | 1.73 | 1.96 | 1.81 |
| AP | .47 | .48 | .46 | .48 | .47 | .49 | .48 |

JUAN DE FUCA RIDGE BASALTS (CONT.)

| Sample # | 4-6 | 4-8 | 5-3 | 5-5 | 5-10 | 5-12 | 6-5 |
|--------------------------------|------|------|------|------|------|------|------|
| SiO ₂ | 50.8 | 50.3 | 49.8 | 51.1 | 50.0 | 51.0 | 49.6 |
| Al ₂ O ₃ | 14.5 | 14.2 | 14.2 | 13.9 | 13.8 | 14.0 | 13.8 |
| CaO | 11.6 | 11.5 | 12.0 | 11.4 | 12.5 | 11.2 | 10.9 |
| MgO | 7.6 | 7.61 | 8.01 | 7.09 | 7.25 | 7.26 | 6.71 |
| K ₂ O | .19 | .19 | .13 | .15 | .16 | .14 | .22 |
| Na ₂ O | 2.45 | 2.30 | 2.27 | 2.52 | 2.44 | 2.44 | 2.54 |
| FeO* | 10.5 | 10.7 | 10.0 | 10.0 | 10.2 | 11.1 | 10.9 |
| TiO ₂ | 1.68 | 1.69 | 1.55 | 1.71 | 1.66 | 1.96 | 2.24 |
| TOTAL | 99.4 | 98.7 | 98.0 | 98.0 | 98.2 | 99.1 | 97.0 |
| Sc | 42 | 40 | 39 | 42 | 42 | 42 | 41 |
| Cr | 240 | 221 | 326 | 202 | 212 | 213 | 152 |
| Ni | 81 | 78 | 80 | 67 | 60 | 69 | 60 |
| Co | 46 | 43 | 46 | 44 | 46 | 45 | 43 |
| Cu | 53 | 57 | 60 | 69 | 67 | 47 | 75 |

CIPW NORMS

| | | | | | | | |
|-----|-------|-------|-------|-------|-------|-------|-------|
| QTZ | .03 | 1.10 | --- | 1.84 | --- | 1.49 | 1.45 |
| NE | --- | --- | --- | --- | --- | --- | --- |
| OR | 1.12 | 1.14 | .78 | .90 | .96 | .83 | 1.33 |
| AB | 20.74 | 19.81 | 18.48 | 21.64 | 20.91 | 20.72 | 21.17 |
| AN | 28.09 | 28.49 | 28.79 | 26.59 | 26.62 | 26.93 | 26.83 |
| DI | 23.05 | 23.38 | 24.82 | 24.39 | 28.64 | 22.67 | 22.36 |
| HY | 21.43 | 20.58 | 19.38 | 19.06 | 16.17 | 21.23 | 19.91 |
| OL | --- | --- | 1.49 | --- | 1.18 | --- | --- |
| IL | 3.19 | 3.27 | 2.99 | 3.30 | 3.19 | 3.68 | 4.36 |
| MT | 1.89 | 1.77 | 1.81 | 1.83 | 1.87 | 1.99 | 2.02 |
| AP | .47 | .48 | .48 | .48 | .48 | .48 | .49 |

JUAN DE FUCA AND GORDA RIDGE BASALTS (CONT.)

| Sample # | A-1A | A-1B | A-4-16 | 0700 | 1145C | 1145K | 1755B |
|--------------------------------|------|------|--------|------|-------|-------|-------|
| SiO ₂ | 49.7 | 51.7 | 51.8 | 50.0 | 51.0 | 53.1 | 50.7 |
| Al ₂ O ₃ | 13.7 | 13.7 | 13.8 | 17.0 | 15.3 | 14.5 | 15.5 |
| CaO | 10.8 | 10.7 | 9.8 | 11.4 | 12.3 | 11.7 | 11.8 |
| MgO | 6.52 | 6.63 | 8.00 | 6.63 | 6.99 | 7.34 | 7.07 |
| K ₂ O | .20 | .21 | .17 | .18 | .17 | .12 | .15 |
| Na ₂ O | 2.62 | 2.56 | 2.78 | 2.74 | 2.44 | 2.44 | 2.41 |
| FeO* | 11.6 | 11.4 | 10.7 | 8.2 | 7.7 | 8.3 | 7.6 |
| TiO ₂ | 2.05 | 2.03 | 2.00 | 1.66 | 1.39 | 1.36 | 1.14 |
| TOTAL | 97.3 | 99.1 | 99.2 | 98.0 | 97.5 | 100.1 | 96.5 |
| Sc | 44 | 43 | 34 | 37 | 42 | 36 | 37 |
| Cr | 139 | 131 | 313 | 221 | 337 | 290 | 293 |
| Ni | 44 | 46 | 160 | 108 | 127 | 111 | 100 |
| Co | 46 | 47 | 48 | 39 | 48 | 39 | 38 |
| Cu | 66 | 71 | 65 | 62 | 88 | 66 | 66 |

CIPW NORMS

| | | | | | | | |
|-----|-------|-------|-------|-------|-------|-------|-------|
| QTZ | .44 | 2.79 | 1.35 | --- | 5.31 | 4.12 | 2.59 |
| NE | --- | --- | --- | --- | --- | --- | --- |
| OR | 1.21 | 1.25 | 1.01 | 1.08 | 1.06 | 0.71 | 0.94 |
| AB | 22.65 | 21.73 | 23.57 | 23.54 | 20.52 | 20.73 | 20.69 |
| AN | 25.65 | 25.49 | 24.89 | 34.18 | 30.10 | 28.48 | 30.43 |
| DI | 23.14 | 22.08 | 18.72 | 18.02 | 24.12 | 23.47 | 23.76 |
| HY | 20.34 | 20.28 | 24.28 | 16.92 | 14.43 | 17.92 | 17.36 |
| OL | --- | --- | --- | 1.11 | --- | --- | --- |
| IL | 3.98 | 3.87 | 3.81 | 3.20 | 2.62 | 2.59 | 2.29 |
| MT | 2.13 | 2.07 | 1.92 | 1.50 | 1.38 | 1.51 | 1.46 |
| AP | .48 | .48 | .48 | 0.48 | 0.47 | 0.48 | 0.50 |

GORDA RIDGE BASALTS (CONT.)

| Sample # | 1755E | 1755G | 3-1 | 3-4 | 3-6 | 3-7 | 3-8 |
|--------------------------------|-------|-------|------|------|------|------|------|
| SiO ₂ | 51.6 | 52.0 | 52.0 | 51.0 | 51.6 | 49.9 | 48.4 |
| Al ₂ O ₃ | 15.3 | 15.7 | 14.6 | 15.7 | 15.2 | 16.3 | 16.1 |
| CaO | 12.9 | 11.9 | 11.5 | 11.2 | 11.3 | 11.5 | 11.1 |
| MgO | 7.53 | 7.14 | 8.13 | 7.67 | 7.67 | 7.93 | 7.55 |
| K ₂ O | .07 | .13 | .11 | .12 | .12 | .14 | .13 |
| Na ₂ O | 2.42 | 2.50 | 2.41 | 2.53 | 2.45 | 2.41 | 2.54 |
| FeO* | 7.3 | 7.8 | 8.0 | 8.5 | 8.0 | 8.3 | 8.9 |
| TiO ₂ | 1.18 | 1.45 | 1.37 | 1.56 | 1.49 | 1.50 | 1.60 |
| TOTAL | 98.5 | 98.8 | 98.3 | 98.4 | 98.1 | 97.9 | 96.5 |
| Sc | 39 | 41 | 34 | 35 | 36 | 36 | 36 |
| Cr | 249 | 169 | 296 | 271 | 310 | 288 | 280 |
| Ni | 111 | 86 | 150 | 135 | 132 | 136 | 137 |
| Co | 41 | 43 | 41 | 40 | 40 | 40 | 41 |
| Cu | 71 | 71 | 64 | 66 | 66 | 71 | 68 |

CIPW NORMS

| | | | | | | | |
|-----|-------|-------|-------|-------|-------|-------|-------|
| QTZ | 0.63 | 1.20 | 2.41 | 0.97 | 2.43 | --- | --- |
| NE | --- | --- | --- | --- | --- | --- | --- |
| OR | 0.36 | 0.74 | 0.66 | 0.72 | 0.72 | 0.84 | 0.79 |
| AB | 19.99 | 21.96 | 20.62 | 21.63 | 21.02 | 20.71 | 22.15 |
| AN | 34.95 | 29.76 | 29.21 | 31.62 | 30.74 | 33.79 | 33.25 |
| DI | 21.82 | 24.51 | 22.34 | 19.18 | 20.47 | 18.52 | 18.09 |
| HY | 18.12 | 17.09 | 20.20 | 20.89 | 19.83 | 19.89 | 15.39 |
| OL | --- | --- | --- | --- | --- | 1.42 | 5.06 |
| IL | 2.32 | 2.82 | 2.63 | 2.99 | 2.87 | 2.87 | 3.13 |
| MT | 1.34 | 1.46 | 1.47 | 1.54 | 1.47 | 1.50 | 1.66 |
| AP | 0.48 | 0.49 | 0.48 | 0.48 | 0.48 | 0.48 | 0.49 |

GORDA RIDGE BASALTS (CONT.)

| Sample # | 3-10 | 4-7 | 4-10 | 4-12 | 4-15 | 4-26 | 4-29 |
|--------------------------------|------|------|------|------|------|------|------|
| SiO ₂ | 50.3 | 50.4 | 49.7 | 50.0 | 52.5 | 52.1 | 50.8 |
| Al ₂ O ₃ | 14.6 | 15.4 | 14.9 | 14.6 | 14.3 | 14.3 | 14.6 |
| CaO | 10.4 | 11.3 | 10.3 | 11.1 | 11.1 | 11.1 | 11.1 |
| MgO | 7.09 | 7.13 | 6.33 | 7.49 | 7.66 | 7.73 | 8.05 |
| K ₂ O | .12 | .10 | .14 | .13 | .17 | .13 | .16 |
| Na ₂ O | 2.53 | 2.51 | 2.89 | 2.67 | 2.59 | 2.69 | 2.70 |
| FeO* | 8.4 | 8.9 | 10.2 | 8.9 | 8.9 | 8.1 | 8.8 |
| TiO ₂ | 1.60 | 1.41 | 2.21 | 1.60 | 1.63 | 1.52 | 1.56 |
| TOTAL | 95.2 | 97.3 | 96.9 | 96.8 | 99.0 | 97.8 | 98.0 |
| Sc | 34 | 37 | 38 | 41 | 42 | 39 | 41 |
| Cr | 284 | 285 | 146 | 289 | 295 | 274 | 291 |
| Ni | 129 | 115 | 76 | 91 | 94 | 93 | 07 |
| Co | 41 | 39 | 40 | 40 | 42 | 39 | 41 |
| Cu | 65 | 75 | 58 | 72 | 72 | 72 | 73 |

CIPW NORMS

| | | | | | | | |
|-----|-------|-------|-------|-------|-------|-------|-------|
| QTZ | 6.19 | 3.17 | 0.57 | --- | 2.76 | 2.41 | --- |
| NE | --- | --- | --- | --- | --- | --- | --- |
| OR | 0.76 | 0.64 | 0.85 | 0.79 | 1.01 | 0.78 | 0.96 |
| AB | 22.87 | 22.89 | 25.10 | 23.22 | 22.03 | 23.14 | 23.19 |
| AN | 26.17 | 27.09 | 28.21 | 28.26 | 27.25 | 27.17 | 27.82 |
| DI | 19.68 | 21.90 | 18.96 | 22.25 | 21.84 | 22.54 | 21.54 |
| HY | 10.01 | 19.40 | 19.64 | 19.53 | 19.95 | 19.08 | 20.53 |
| OL | --- | --- | --- | 0.72 | --- | --- | 0.54 |
| IL | 3.21 | 2.89 | 4.31 | 3.12 | 3.11 | 2.94 | 3.03 |
| MT | 1.61 | 1.53 | 1.89 | 1.64 | 1.60 | 1.47 | 1.62 |
| AP | 0.51 | 0.51 | 0.49 | 0.49 | 0.48 | 0.48 | 0.48 |

GORDA RIDGE BASALTS (CONT.)

| Sample # | 4-62 | 5-9 | 5-10 | 5-16 | 5-18 | 5-22 | 5-23 |
|--------------------------------|------|------|-------|------|------|------|------|
| SiO ₂ | 49.4 | 51.0 | 51.5 | 49.7 | 51.2 | 51.2 | 49.8 |
| Al ₂ O ₃ | 15.1 | 14.2 | 17.4 | 16.2 | 16.4 | 15.4 | 15.7 |
| CaO | 11.7 | 11.1 | 13.0 | 11.7 | 11.9 | 11.6 | 11.3 |
| MgO | 7.42 | 6.69 | 7.13 | 7.20 | 6.78 | 7.26 | 7.11 |
| K ₂ O | .09 | .10 | .13 | .14 | .12 | .14 | .15 |
| Na ₂ O | 2.28 | 2.44 | 2.60 | 2.67 | 2.59 | 2.68 | 2.60 |
| FeO* | 8.9 | 8.4 | 7.8 | 8.6 | 8.0 | 8.4 | 8.6 |
| TiO ₂ | 1.21 | 1.43 | 1.42 | 1.57 | 1.43 | 1.54 | 1.56 |
| TOTAL | 95.4 | 95.5 | 101.1 | 97.9 | 98.6 | 98.3 | 96.9 |
| Sc | 37 | 39 | 35 | 41 | 37 | 40 | 40 |
| Cr | 329 | 199 | 207 | 217 | 223 | 199 | 208 |
| Ni | 120 | 87 | 194 | 93 | 90 | 92 | 86 |
| Co | 42 | 65 | 38 | 43 | 39 | 41 | 41 |
| Cu | 72 | 64 | 63 | 70 | 67 | 64 | 69 |

CIPW NORMS

| | | | | | | | |
|-----|-------|-------|-------|-------|-------|-------|-------|
| QTZ | 1.02 | 4.05 | --- | --- | 1.21 | 0.86 | 0.05 |
| NE | --- | --- | --- | --- | --- | --- | --- |
| OR | 0.56 | 0.62 | 0.74 | 0.84 | 0.72 | 0.84 | 0.91 |
| AB | 20.12 | 21.49 | 21.23 | 22.94 | 22.11 | 22.94 | 22.57 |
| AN | 32.13 | 28.62 | 39.44 | 32.54 | 33.14 | 29.94 | 31.60 |
| DI | 22.27 | 22.57 | 17.68 | 20.45 | 20.85 | 22.20 | 20.10 |
| HY | 19.52 | 17.77 | 11.96 | 14.81 | 17.32 | 18.17 | 19.68 |
| OL | --- | --- | 4.54 | 3.33 | --- | --- | --- |
| IL | 2.40 | 2.83 | 2.60 | 3.05 | 2.74 | 2.96 | 3.04 |
| MT | 1.50 | 1.59 | 1.36 | 1.58 | 1.46 | 1.53 | 1.59 |
| AP | 0.49 | 0.49 | 0.46 | 0.48 | 0.48 | 0.48 | 0.49 |

GORDA RIDGE BASALTS (CONT.)

| Sample # | 5-25 | 5-26 | 5-29 | 5-37 | Precision: maximum errors for each oxides (wt. %) |
|--------------------------------|------|------|------|------|---|
| SiO ₂ | 50.8 | 51.1 | 52.0 | 49.6 | ± .79 |
| Al ₂ O ₃ | 14.9 | 15.5 | 14.6 | 15.4 | ± .71 |
| CaO | 11.5 | 11.6 | 10.8 | 12.4 | ± .22 |
| MgO | 7.45 | 7.47 | 7.48 | 6.49 | ± .18 |
| K ₂ O | .14 | .12 | .14 | .06 | ± .004 |
| Na ₂ O | 2.53 | 2.47 | 2.50 | 2.62 | ± .14 |
| FeO* | 9.0 | 8.0 | 9.4 | 8.6 | ± .60 |
| TiO ₂ | 1.55 | 1.33 | 1.55 | 1.54 | ± .02 |
| TOTAL | 98.0 | 97.8 | 98.5 | 96.8 | Maximum error (in ppm) |
| Sc | 42 | 38 | 43 | 43 | ± 2 |
| Cr | 212 | 273 | 218 | 221 | ± 3 |
| Ni | 81 | 107 | 87 | 98 | ± 2 |
| Co | 42 | 39 | 44 | 44 | ± 3 |
| Cu | 68 | 65 | 68 | 71 | ± 5 |

CIPW NORMS

| | | | | |
|-----|-------|-------|-------|-------|
| QTZ | 0.83 | 1.53 | 2.87 | --- |
| NE | --- | --- | --- | --- |
| OR | 0.84 | 0.72 | 0.84 | 0.36 |
| AB | 21.72 | 21.26 | 21.36 | 22.77 |
| AN | 29.45 | 31.41 | 28.48 | 30.98 |
| DI | 22.27 | 21.33 | 19.92 | 25.55 |
| HY | 19.79 | 19.24 | 21.39 | 15.03 |
| OL | --- | --- | --- | 0.25 |
| IL | 2.99 | 2.57 | 2.97 | 3.00 |
| MT | 1.65 | 1.46 | 1.70 | 1.58 |
| AP | 0.48 | 0.48 | 0.48 | 0.49 |

APPENDIX B. INSTRUMENTAL NEUTRON ACTIVATION ANALYSIS
FOR RARE EARTH ELEMENTAL ABUNDANCES.

The REE abundances for Juan de Fuca and Gorda Ridge basalts are listed as weight parts per million.

REE ABUNDANCES OF JUAN DE FUCA RIDGE BASALTS

| Sample # | LA | CE | SM | EU | TB | YB | LU | HF |
|----------|-----|------|------|------|------|-----|-----|------|
| Y74-1-8 | 3.0 | 8.2 | 3.06 | 1.18 | .77 | 3.4 | .57 | 1.49 |
| Y74-1-9 | 2.1 | 5.7 | 2.91 | .99 | .72 | 2.6 | .52 | 1.67 |
| Y74-1-49 | 3.0 | 7.4 | 2.86 | 1.09 | .65 | 3.2 | .40 | 1.32 |
| Y74-1-55 | 3.1 | 7.7 | 3.22 | 1.26 | .89 | 3.1 | .65 | 2.01 |
| Y74-2-3 | 3.6 | 9.3 | 3.21 | 1.30 | .92 | 3.6 | .41 | 2.25 |
| Y74-2-4 | 2.6 | 5.4 | 2.98 | .84 | .79 | 3.2 | .48 | 1.27 |
| Y74-2-6 | 3.0 | 10.2 | 3.51 | 1.08 | .84 | 3.3 | .49 | 1.87 |
| Y74-2-12 | 3.8 | 11.5 | 3.15 | 1.28 | .82 | 3.8 | .56 | 2.25 |
| Y74-3-5 | 1.2 | 4.8 | 1.73 | .61 | .50 | 1.7 | .34 | .41 |
| Y74-3-13 | 1.2 | 4.6 | 1.46 | .96 | .54 | 3.0 | .28 | 1.18 |
| Y74-3-23 | 4.6 | 12.7 | 3.97 | 1.20 | 1.04 | 2.7 | .39 | 2.56 |
| Y74-3-29 | 1.4 | 4.8 | 1.65 | .61 | .37 | 2.7 | .33 | 1.11 |
| Y74-4-2 | 5.3 | 13.6 | 4.53 | 1.35 | 1.10 | 4.1 | .53 | 2.89 |
| Y74-4-3 | 5.1 | 12.9 | 3.66 | 1.33 | 1.02 | 3.4 | .51 | 2.24 |
| Y74-4-6 | 4.5 | 12.0 | 3.58 | 1.25 | .93 | 3.6 | .61 | 2.35 |
| Y74-4-8 | 4.5 | 13.6 | 4.09 | .96 | .87 | 3.5 | .37 | 2.77 |
| Y74-5-3 | 3.2 | 11.2 | 3.16 | 1.22 | .78 | 3.0 | .51 | 1.63 |
| Y74-5-5 | 3.9 | 11.2 | 3.52 | 1.18 | .83 | 4.0 | .61 | 1.74 |

REE ABUNDANCES OF JUAN DE FUCA RIDGE BASALTS (CONT.)

| Sample # | LA | CE | SM | EU | TB | YB | LU | HF |
|-------------|-----|------|------|------|------|-----|-----|------|
| Y74-5-10 | 3.8 | 9.3 | 3.93 | 1.14 | .85 | 3.5 | .40 | 1.92 |
| Y74-5-12 | 4.6 | 12.4 | 4.19 | 1.36 | 1.02 | 4.6 | .59 | 2.65 |
| Y74-6-5 | 6.3 | 12.6 | 5.34 | 1.60 | 1.24 | 4.4 | .61 | 3.81 |
| Y74-6-9 | 5.0 | 13.8 | 4.45 | 1.38 | 1.08 | 3.6 | .48 | 3.10 |
| Y74-6-10 | 7.0 | 18.1 | 5.37 | 1.50 | 1.20 | 4.1 | .79 | 3.24 |
| Y74-6-16 | 5.4 | 16.4 | 4.90 | 1.53 | 1.42 | 4.1 | .58 | 3.79 |
| Y74-7-1 | 5.7 | 17.9 | 5.21 | 1.68 | 1.45 | 5.3 | .85 | 4.01 |
| Y74-7-2 | 6.3 | 18.1 | 5.88 | 1.59 | 1.50 | 5.1 | .89 | 4.23 |
| Y74-7-6 | 5.8 | 16.1 | 5.29 | 1.74 | 1.30 | 4.8 | .87 | 3.95 |
| Y74-7-9 | 6.6 | 17.4 | 5.92 | 1.84 | 1.21 | 4.8 | .84 | 3.79 |
| Y7305A-1A | 5.5 | 15.7 | 4.81 | 1.77 | 1.12 | 5.0 | .80 | 3.27 |
| Y7305A-1B | 5.8 | 17.1 | 4.85 | 1.79 | 1.20 | 5.1 | .67 | 3.32 |
| Y7305A-4-16 | 5.1 | 14.0 | 4.84 | 1.44 | 1.07 | 3.7 | .55 | 3.15 |

REE ABUNDANCES OF GORDA RIDGE BASALTS

| Sample # | LA | CE | SM | EU | TB | YB | LU | HF |
|-------------|-----|------|------|------|------|-----|-----|------|
| W7605B-3-1 | 4.0 | 10.9 | 2.91 | 1.17 | .81 | 3.0 | .38 | 2.14 |
| W7605B-3-4 | 4.1 | 12.6 | 3.48 | 1.17 | .92 | 2.8 | .53 | 2.93 |
| W7605B-3-6 | 4.0 | 11.0 | 3.16 | 1.05 | .84 | 3.1 | .45 | 2.32 |
| W7605B-3-7 | 3.5 | 11.2 | 3.01 | 1.19 | .98 | 3.1 | .45 | 2.25 |
| W7605B-3-8 | 3.5 | 12.9 | 3.63 | 1.44 | 1.06 | 2.6 | .51 | 3.14 |
| W7605B-3-10 | 4.2 | 12.0 | 3.46 | 1.36 | 1.03 | 3.5 | .54 | 2.84 |
| W7605B-4-7 | 2.6 | 9.8 | 3.09 | 1.30 | .75 | 2.5 | .36 | 2.27 |
| W7605B-4-10 | 5.4 | 16.0 | 5.00 | 1.65 | 1.43 | 4.5 | .64 | 3.83 |
| W7605B-4-12 | 3.6 | 12.1 | 3.58 | 1.33 | 1.07 | 3.4 | .45 | 2.92 |
| W7605B-4-15 | 3.9 | 11.7 | 3.67 | 1.32 | 1.07 | 2.9 | .46 | 2.50 |
| W7605B-4-26 | 3.4 | 9.8 | 3.08 | 1.15 | .80 | 2.6 | .33 | 2.24 |
| W7605B-4-29 | 3.8 | 11.0 | 3.55 | 1.34 | .94 | 3.1 | .43 | 2.49 |
| W7605B-4-62 | 3.1 | 7.7 | 2.46 | 1.04 | .75 | 2.7 | .36 | 2.07 |
| W7605B-5-9 | 2.0 | 8.2 | 3.09 | 1.12 | .89 | 2.9 | .47 | 2.24 |
| W7605B-5-10 | 3.2 | 8.4 | 2.86 | 1.23 | .68 | 3.0 | .37 | 1.98 |
| W7605B-5-16 | 3.4 | 9.3 | 3.23 | 1.26 | .91 | 2.7 | .29 | 2.45 |
| W7605B-5-18 | 3.0 | 9.1 | 2.94 | 1.04 | .77 | 2.8 | .41 | 2.00 |
| W7605B-5-22 | 3.5 | 9.5 | 3.26 | 1.11 | .95 | 2.7 | .39 | 1.96 |

REE ABUNDANCES OF GORDA RIDGE BASALTS (CONT.)

| SAMPLE # | LA | CE | SM | EU | TB | YB | LU | HF |
|-------------|-----|------|------|------|------|-----|-----|------|
| W7605B-5-23 | 3.4 | 9.8 | 3.16 | 1.25 | .92 | 3.4 | .51 | 2.34 |
| W7605B-5-25 | 2.9 | 9.5 | 3.39 | 1.21 | .88 | 2.6 | .54 | 2.51 |
| W7605B-5-26 | 1.9 | 8.4 | 2.66 | 1.01 | .82 | 2.3 | .47 | 2.42 |
| W7605B-5-29 | 2.8 | 9.9 | 3.23 | 1.37 | 1.10 | 3.1 | .49 | 2.45 |
| W7605B-5-37 | 2.4 | 9.2 | 3.08 | 1.21 | .88 | 3.4 | .42 | 1.92 |
| 0700 | 3.5 | 11.1 | 3.66 | 1.20 | .90 | 3.3 | .51 | 2.86 |
| 1145C | 3.0 | 9.6 | 2.92 | 1.27 | .76 | 3.1 | .53 | 2.29 |
| 1145K | 2.6 | 7.9 | 2.75 | 1.12 | .90 | 2.7 | .45 | 2.20 |
| 1755B | 2.4 | 6.6 | 2.35 | .93 | .69 | 2.1 | .26 | 1.51 |
| 1755E | 2.6 | 7.0 | 2.37 | .79 | .82 | 2.6 | .46 | 1.50 |
| 1755G | 3.0 | 8.7 | 3.13 | 1.20 | 1.00 | 3.1 | .46 | 1.79 |

 Range of estimated errors due INAA counting statistics:

Sm: 1-5%; La, Eu, Yb, Lu, Hf: 5-10%; Tb: 10-15%; Ce: 5-15%

APPENDIX C. CHEMICAL ANALYSES OF STANDARD ROCKS
COMPARED TO PUBLISHED RESULTS

1. Accuracy for instrumental neutron activation analysis based on comparison of analytical results with standards, SRW1, SRCRB, SD0895, and MS1519.

2. Accuracy for atomic absorption spectrophotometric analysis based on comparison of analytical results with standard SRW1.

C-1. CHEMICAL ANALYSES OF STANDARD ROCKS COMPARED TO PUBLISHED RESULTS (in ppm)

| | SRW1 | SRW1* | SRCRB | SRCRB* | SD0895 | SD0895+ | MS1519 | MS1519+ |
|-------------------|--------|--------|-------|--------|--------|---------|--------|---------|
| Na ₂ O | 2.24 | 2.15 | 3.13 | 3.27 | 1.48 | 1.54 | 5.94 | 6.01 |
| FeO* | 10.05 | 9.98 | 12.15 | 12.06 | 6.88 | 6.93 | 14.44 | 15.17 |
| Sc | 35.45 | 35.10 | 30.64 | 33.00 | 22.05 | 24.20 | 20.89 | 23.70 |
| Cr | 129.90 | 114.00 | 10.01 | 17.60 | 97.35 | 97.10 | 21.76 | 23.70 |
| Co | 49.28 | 47.00 | 38.77 | 38.00 | 140.10 | 137.40 | 200.07 | 192.80 |
| La | 10.06 | 9.80 | 26.14 | 26.00 | 68.80 | 71.90 | 184.40 | 187.40 |
| Ce | 23.29 | 23.00 | 50.43 | 53.90 | 135.41 | 119.50 | 71.94 | 67.60 |
| Sm | 3.57 | 3.60 | 6.98 | 6.60 | 18.79 | 18.80 | 34.80 | 34.40 |
| Eu | 1.08 | 1.11 | 1.93 | 1.94 | 3.87 | 4.40 | 8.97 | 9.10 |
| Tb | 0.69 | 0.65 | 1.38 | 1.00 | 3.51 | 2.90 | 8.03 | 5.30 |
| Yb | 2.31 | 2.10 | 3.45 | 3.36 | 7.82 | 7.80 | 29.73 | 30.60 |
| Lu | 0.30 | 0.35 | 0.57 | 0.55 | 1.17 | 1.20 | 4.60 | 4.90 |
| Hf | 2.53 | 2.67 | 4.49 | 4.70 | 4.74 | 4.90 | 3.97 | 4.10 |

* published data (Flanagan, 1969)

+ laboratory standards (School of Oceanography)

Na₂O and FeO* in wt. % oxide

C-2. CHEMICAL ANALYSES OF STANDARD ROCKS COMPARED TO PUBLISHED RESULTS (in wt. % oxides).

| | <u>SRW1</u> | <u>SRW1*</u> |
|--------------------------------|-------------|--------------|
| SiO ₂ | 52.37 | 52.64 |
| Al ₂ O ₃ | 14.94 | 15.00 |
| MgO | 6.51 | 6.62 |
| CaO | 10.50 | 10.96 |
| K ₂ O | 0.62 | 0.64 |
| TiO ₂ | 1.11 | 1.07 |
| Cu (ppm) | 121.19 | 110.00 |
| Ni (ppm) | 71.87 | 76.00 |

* published data (Flanagan, 1969)

APPENDIX D. RESULTS FROM PETROGRAPHIC ANALYSIS.

The following are abbreviated forms for the presence of crystals: PL = plagioclase, OL = olivine, CPX = clinopyroxene. Phenocrysts are crystals whose dimension measures greater than 0.5 mm. Microphenocrysts are well-defined crystals whose dimension measures less than 0.5 mm. However, it is still greater than the dimension of groundmass microlites which are more difficult to identify mineralogically. Vesicularity implies presence (Yes) or absence (No or rare) of vesicles observed in thin sections. Remarks will include comments on occurrence of resorption, of oscillatory zoning, presence of chrome spinels, and signs of alteration wherever noted.

PETROGRAPHY OF JUAN DE FUCA RIDGE BASALTS

| Sample No. | Phenocrysts | Microphenocrysts | Microlites | Vesicularity | Remarks |
|------------|-------------|------------------|------------|--------------|---|
| Y74-1-8 | | | PL | yes | Fe-Ti oxides |
| Y74-1-9 | | | PL | yes | Fe-Ti oxides |
| Y74-1-49 | | | PL | yes | Fe-Ti oxides slightly altered |
| Y74-1-55 | PL | PL, OL, CPX | | yes | rare PL: zoned OL: euhedral, skeletal PL: skeletal inter- growth w/ OL Fe-Ti oxides |
| Y74-2-3 | | PL, OL, CPX | PL | yes | rare PL: resorbed OL: euhedral, skeletal Fe-Ti oxides |
| Y74-2-4 | | PL, OL, CPX | PL | yes | PL: skeletal OL: euhedral, skeletal CPX: intergrowth w/ PL Fe-Ti oxides |
| Y74-2-6 | PL | PL, OL, CPX | | yes | rare PL: resorbed CPX: intergrowth w//PL Fe-Ti oxides slightly altered |

PETROGRAPHY OF JUAN DE FUCA RIDGE BASALTS (CONT.)

| Sample No. | Phenocrysts | Microphenocrysts | Microlites | Vesicularity | Remarks |
|------------|-------------|------------------|------------|--------------|---|
| Y74-2-12 | PL | PL, OL, CPX | | yes | rare PL: resorbed, zoned OL: euhedral, skeletal Fe-Ti oxides slightly altered |
| Y74-3-5 | | OL | PL | rare | OL: resorbed abundant Cr-spinel no Fe-Ti in groundmass |
| Y74-3-13 | PL | OL | PL | rare | OL: resorbed, rounded PL: rare abundant Cr-spinel minor Fe-Ti oxides |
| Y74-3-23 | PL | PL, CPX | PL | yes | rare PL: resorbed, zoned CPX: intergrowth w/ PL Fe-Ti oxides |
| Y74-3-29 | PL | OL | PL | rare | OL: resorbed, rounded PL: rare abundant Cr-spinel no Fe-Ti oxides |

PETROGRAPHY OF JUAN DE FUCA RIDGE BASALTS (CONT.)

| Sample No. | Phenocrysts | Microphenocrysts | Microlites | Vesicularity | Remarks |
|------------|-------------|------------------|------------|--------------|--|
| Y74-4-2 | | PL, OL, CPX | PL | yes | PL: zoned OL: rare Fe-Ti oxides |
| Y74-4-3 | PL | | PL | yes | PL: rare Fe-Ti oxides |
| Y74-4-6 | | | PL | yes | rare Fe-Ti oxides |
| Y74-4-8 | | PL | PL | yes | Fe-Ti oxides |
| Y74-5-3 | PL | PL, OL, CPX | PL | yes | PL: resorbed, zoned OL: euhedral, skeletal CPX: intergrowth w/ PL Fe-Ti oxides rare Cr-spinel |
| Y74-5-5 | | PL, OL, CPX | PL | yes | OL: resorbed CPX: intergrowth w/ PL slightly altered |

PETROGRAPHY OF JUAN DE FUCA RIDGE BASALTS (CONT.)

| Sample No. | Phenocrysts | Microphenocrysts | Microlites | Vesicularity | Remarks |
|------------|-------------|------------------|------------|--------------|--|
| Y74-5-10 | PL, OL | PL, OL, CPX | PL | yes | PL: zoned OL: euhedral, skeletal CPX: intergrowth w/ PL Fe-Ti oxides rare Cr-spinel slightly altered |
| Y74-5-12 | PL | PL, OL | | yes | PL: resorbed, zoned OL: euhedral, skeletal |
| Y74-6-5 | PL, OL | PL, OL, CPX | PL | yes | OL: euhedral, large CPX: intergrowth w/ PL Fe-Ti oxides slightly altered |
| Y74-6-9 | | PL, CPX | PL | yes | CPX: intergrowth w/ PL Fe-Ti oxides |
| Y74-6-10 | PL, CPX | PL, OL, CPX | PL | yes | PL: resorbed Fe-Ti oxides |

PETROGRAPHY OF JUAN DE FUCA RIDGE BASALTS (CONT.)

| Sample No. | Phenocrysts | Microphenocrysts | Microlites | Vesicularity | Remarks |
|------------|-------------|------------------|------------|--------------|--|
| Y74-6-16 | PL, OL | PL, OL | PL | yes | PL: resorbed, zoned OL: resorbed rare opaque magnetite? |
| Y74-7-1 | | PL | PL | yes | PL: rare Fe-Ti oxides |
| Y74-7-2 | | PL, OL, CPX | PL | yes | PL: resorbed, zoned OL: euhedral, skeletal CPX: intergrowth w/ PL |
| Y74-7-6 | | PL | PL | yes | PL: rare, zoned Fe-Ti oxides slightly altered |
| Y74-7-9 | | PL, OL, CPX | PL | yes | CPX: intergrowth w/ PL Fe-Ti oxides |
| Y7305A-1A | PL | PL, OL, CPX | | yes | PL: resorbed, zoned slightly holocrystalline |
| Y7305A-1B | | PL, OL, CPX | | yes | also crystalline PL: resorbed |

PETROGRAPHY OF JUAN DE FUCA AND GORDA RIDGE BASALTS (CONT.)

| Sample No. | Phenocrysts | Microphenocrysts | Microlites | Vesicularity | Remarks |
|-------------|-------------|------------------|------------|--------------|--|
| Y7305A-4-16 | | PL, OL, CPX | PL | yes | OL: some euhedral OL: resorbed CPX: intergrowth w/ PL rare Cr-spinel |
| W7605B-3-1 | PL | PL, OL | PL | yes | PL: resorbed, zoned OL: resorbed slightly altered |
| W7605B-3-4 | PL, OL | PL | PL | yes | PL: resorbed, zoned OL: resorbed |
| W7605B-3-6 | PL, OL | PL | PL | yes | PL: abundant OL: resorbed Fe-Ti oxides rare Cr-spinel |
| W7605B-3-7 | PL, OL | PL, OL | PL | yes | PL: abundant OL: resorbed OL: some euhedral, skeletal Fe-Ti oxides |
| W7605B-3-8 | PL, OL | PL, OL | PL | yes | PL: resorbed OL: euhedral |

PETROGRAPHY OF JUAN DE FUCA AND GORDA RIDGE BASALTS (CONT.)

| Sample No. | Phenocrysts | Microphenocrysts | Microlites | Vesicularity | Remarks |
|-------------|-------------|------------------|------------|--------------|--|
| W7605B-3-10 | PL, OL | PL | PL | yes | PL: resorbed OL: resorbed rare Cr-spinel |
| W7605B-4-7 | PL | PL, OL | PL | yes | OL: euhedral, skeletal |
| W7605B-4-10 | PL | PL, OL, CPX | PL | yes | PL: resorbed, zoned OL: euhedral, skeletal CPX: intergrowth w/ PL |
| W7605B-4-12 | PL, OL | PL, OL | PL | yes | PL: resorbed, zoned PL: some skeletal OL: euhedral, skeletal slightly altered |
| W7605B-4-15 | PL | PL, OL | PL | yes | PL: resorbed, zoned PL: some skeletal OL: euhedral, skeletal Fe-Ti oxides |
| W7605B-4-26 | PL | PL, OL, CPX | PL | yes | PL: skeletal OL: skeletal CPX: intergrowth w/ PL Fe-Ti oxides |

PETROGRAPHY OF JUAN DE FUCA AND GORDA RIDGE BASALTS (CONT.)

| Sample No. | Phenocrysts | Microphenocrysts | Microlites | Vesicularity | Remarks |
|-------------|-------------|------------------|------------|--------------|--|
| W7605B-4-29 | | PL, OL, CPX | PL | yes | PL: skeletal Fe-Ti oxides slightly altered |
| W7605B-4-62 | PL | PL, OL | PL | yes | PL: resorbed, zoned OL: euhedral |
| W7605B-5-9 | PL | PL, OL, CPX | PL | yes | OL: resorbed, rounded Fe-Ti oxides |
| W7605B-5-10 | PL, OL | PL, OL | PL | yes | OL: rounded rare Cr-spinel |
| W7605B-5-16 | PL | PL, OL | PL | yes | PL: resorbed, zoned OL: resorbed |
| W7605B-5-18 | PL, OL | PL, OL | PL | yes | PL: abundant |
| W7605B-5-22 | PL, OL | PL | PL | yes | PL: abundant |
| W7605B-5-23 | PL, OL | PL | PL | yes | PL: abundant OL: rare, resorbed |
| W7605B-5-25 | PL, OL | PL, OL | PL | yes | PL: abundant slightly altered |

PETROGRAPHY OF JUAN DE FUCA AND GORDA RIDGE BASALTS (CONT.)

| Sample No. | Phenocrysts | Microphenocrysts | Microlites | Vesicularity | Remarks |
|-------------|-------------|------------------|------------|--------------|---|
| W7605B-5-26 | PL, OL | PL, OL | PL | yes | PL: abundant OL: resorbed OL: euhedral, skeletal slightly altered |
| W7605B-5-29 | PL | PL, OL | PL | yes | Fe-Ti oxides slightly altered |
| W7605B-5-37 | PL, OL | PL, OL, CPX | | yes | holocrystalline Fe-Ti oxides |
| 0700 | PL | PL, OL, CPX | PL | yes | PL: abundant Fe-Ti oxides |
| 1145C | PL | PL, OL | PL | yes | PL: abundant OL: euhedral Fe-Ti oxides slightly altered |
| 1145K | PL | | PL | yes | PL: abundant Fe-Ti oxides rare Cr-spinel |
| 1755B | PL, OL | PL, OL | PL | yes | PL: resorbed, zoned OL: euhedral, skeletal Fe-Ti oxides slightly altered |

PETROGRAPHY OF JUAN DE FUCA AND GORDA RIDGE BASALTS (CONT.)

| Sample No. | Phenocrysts | Microphenocrysts | Microlites | Vesicularity | Remarks |
|------------|-------------|------------------|------------|--------------|--|
| 1755E | PL, OL | PL, OL | PL | yes | slightly crystalline moderately altered |
| 1755G | PL | PL, OL | PL | yes | Fe-Ti oxides |